

Possible phases of two coupled n -component fermionic chains

E. Szirmai and J. Sólyom

Research Institute for Solid State Physics and Optics, H-1525 Budapest, P.O.Box 49, Hungary

(Dated: March 23, 2022)

A two-leg ladder with n -component fermionic fields in the chains has been considered using an analytic renormalization group method. The fixed points and possible phases have been determined for generic filling as well as for a half-filled system and for the case when one of the subbands is half filled. A weak-coupling Luttinger-liquid phase and several strong-coupling gapped phases have been found. In the Luttinger liquid phase, for the most general spin dependence of the couplings, all $2n$ modes have different velocities if the interband scattering processes are scaled out, while n doubly degenerate modes appear if the interband scattering processes remain finite. The role of backward-scattering, charge-transfer and umklapp processes has been analysed using their bosonic form and the possible phases are characterized by the number of gapless modes. As a special case the $SU(n)$ symmetric Hubbard ladder has been investigated numerically. It was found that this model does not scale to the Luttinger liquid fixed point. Even for generic filling gaps open up in the spectrum of the spin or charge modes, and the system is always insulator in the presence of umklapp processes.

PACS numbers: 71.30.+h, 71.10.Fd

I. INTRODUCTION

Recently, systems exhibiting non-Fermi-liquid behavior have been intensively studied, especially in connection with the unusual normal-state properties of high-temperature superconductors. Low-dimensional models are of special interest in this respect due to their possible Luttinger-liquid¹ behavior. The simplest model that has a non-Fermi-liquid ground state is the exactly solvable one-dimensional (1D) Hubbard chain.² Unless the band is half filled, this system is a prototype of Luttinger liquids.

In most strongly correlated systems, the degenerate d or f bands of the transition-metal or rare-earth ions play an important role and the orbital degrees of freedom, too, have to be taken into account. In an obvious although highly simplified generalization of the Hubbard model, it is assumed that the spin and orbital degrees of freedom can be treated as a unified degree of freedom with n possible values. The $SU(n)$ symmetric generalization of the $SU(2)$ symmetric 1D Hubbard model has been studied by several authors^{3,4,5} to check its possible Luttinger-liquid behavior and to study the metal-insulator transition at half filling or $1/n$ filling. It has been found that the behavior is qualitatively different for $n > 2$ and $n = 2$.

The physics is more complicated when—as a first step towards two-dimensional systems—two Hubbard chains or equivalently two Luttinger liquids are coupled by one-particle hopping into a ladder. The first question that has been addressed is the relevance or irrelevance of the interchain hopping. It has been shown^{6,7,8} that for generic filling the 1D Luttinger liquid is unstable with respect to arbitrarily weak transverse single-particle hopping. Either the system becomes Fermi liquid or new types of states may occur. The situation may be different at a special filling where umklapp processes may suppress the single-electron interchain hopping.⁹

A more difficult problem is to decide what these states may be. To answer this question the Hubbard ladder—or more general models with relevant intrachain backward scattering processes, too—have been studied by different analytic and numerical methods like renormalization group in boson^{7,9,10,11,12,13,14} or fermion^{15,16} representation, Monte Carlo simulations^{17,18} or using the density-matrix renormalization group.^{19,20,21,22}

As a possible classification of the new states Balents and Fisher¹² proposed to characterize the phases by the number of gapless charge and spin modes. Since a two-leg ladder with two-component fermions on both legs has two charge and two spin modes, in principle nine phases can be distinguished in this way. They have shown that seven of them may appear in the weak-coupling regime of the Hubbard ladder. The others can be realized in more general models only, which are defined by more coupling constants.

A more complete characterization of the phases can be obtained by investigating the appropriate correlation functions. When only forward scattering processes are allowed for on the chains, for generic filling, the dominant singularity appears in the spin-density and charge-density responses,¹¹ while if backward-scattering processes are also taken into account the two-chain model has predominant d -type pairing fluctuations even for purely repulsive interactions.^{10,11} Similar result, the possibility of density wave or superconductivity has been found in a variational calculation.²³

Similar situation occurs for the half-filled Hubbard ladder. This model has been shown¹³ to scale to the $SO(8)$ Gross-Neveu model which has fully gapped low-lying excitation spectrum. For repulsive interaction the system is a Mott-insulator spin liquid with d -wave pairing correlations. It is interesting to note that if both repulsive and attractive interactions are allowed for, the phase diagram contains four phases related by $SO(5)$ symme-

try, which can be interpreted²⁴ as unifying magnetism and superconductivity. Similar approximate $SO(5)$ symmetry has been found²⁵ at low energies in the repulsive strong-coupling regime of two coupled Tomonaga-Luttinger chains.

The competition of different density-wave or superconducting orders has been studied^{14,26} in a more general model, where besides the one-particle transverse hopping the Coulomb interaction and Heisenberg exchange between sites on the same rungs and along the diagonals of the elementary plaquette as well have been taken into account.

Although the problem of two coupled two-component fermionic chains has been extensively studied, and some results on the two-dimensional $SU(n)$ Hubbard model are known,^{3,27} to the best of our knowledge the properties of two coupled $SU(n)$ symmetric fermionic chains have not been discussed. For this reason, in this paper, we will present the results obtained for a ladder built up from two n -component fermion systems. In this respect this calculation is an extension of our earlier work.⁵ On the other hand, since a two-leg ladder can be treated as a two-band model, and the method applied is the multiplicative renormalization group combined with bosonization treatment, this paper can also be considered as a generalization of Refs. 16 and 12 to n -valued spin.

The model is introduced and the types of interactions are discussed in Sec. II. The next section contains the scaling equations. The behavior of the system in the weak-coupling Tomonaga-Luttinger fixed point and the properties of the gapless Tomonaga-Luttinger phase of the two-band model are analyzed in Sec. IV. Here the calculations are extended to fully anisotropic spin-dependent couplings. The role of the backward, charge-transfer and umklapp scattering processes is discussed in Sec. V, and the possible gapped phases characterized by the number of gapped modes are presented. The numerical results obtained for the Hubbard ladder and for some more general models are presented in Sec. VI. Finally Sec. VII contains a summary of the main results.

II. THE MODEL

The simplest model we consider is a two-leg $SU(n)$ Hubbard ladder in which two identical $SU(n)$ Hubbard chains described by the Hamiltonians

$$\begin{aligned} \mathcal{H}_j = & t \sum_{i=1}^N \sum_{\sigma=1}^n (a_{j,i,\sigma}^\dagger a_{j,i+1,\sigma} + \text{H.c.}) \\ & + \frac{U}{2} \sum_{i=1}^N \sum_{\sigma,\sigma'=1}^n n_{j,i,\sigma} n_{j,i,\sigma'}, \end{aligned} \quad (1)$$

with $j = 1, 2$, are coupled into a ladder by a rung hopping term

$$\mathcal{H}_\perp = t_\perp \sum_{i=1}^N \sum_{\sigma=1}^n (a_{1,i,\sigma}^\dagger a_{2,i,\sigma} + a_{2,i,\sigma}^\dagger a_{1,i,\sigma}). \quad (2)$$

The local $U(n)$ symmetry of the interaction term is reduced to global $U(n)$ symmetry by the kinetic energy term. An $SU(n)$ symmetric model is obtained if the overall $U(1)$ phase factor is removed. Although in real space, the Hamiltonian has a particularly simple form, in what follows it will be treated in momentum representation, where it is easier to separate the relevant, irrelevant or marginal components.

A. Kinetic energy

The terms describing the intrachain hopping are diagonal in momentum representation. When the interchain hopping is taken into account, the full kinetic energy is diagonalized by the symmetric and antisymmetric combinations of the operators belonging to the two chains:

$$\begin{aligned} a_{k,\sigma} &\equiv \frac{1}{\sqrt{2}} (a_{1,k,\sigma} + a_{2,k,\sigma}), \\ b_{k,\sigma} &\equiv \frac{1}{\sqrt{2}} (a_{1,k,\sigma} - a_{2,k,\sigma}). \end{aligned} \quad (3)$$

As it is shown in Fig. 1, the spectrum consists of two bands labelled by a and b which are obtained by shifting the dispersion curve of the free chain by $\pm t_\perp$.

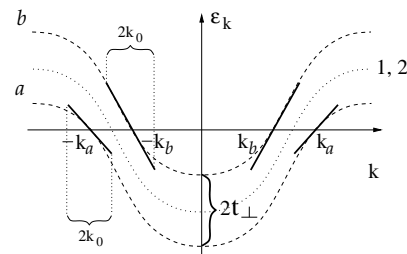


FIG. 1: The spectrum of two coupled chains: the spectrum before (after) hybridization is shown by dotted (dashed) lines. Solid lines indicate the linearized spectrum.

When the number of electrons is small, the upper band is completely empty, and the behavior is identical to that of a one-band Hubbard model. The behavior is similar in the case when the system is close to saturation, and the lower band is completely filled. In what follows it will be assumed that the band filling is between these two extremes, both bands are partially filled, moreover, the Fermi momenta are not too close to the zone center or zone boundary. Under these circumstances one can assume—as is done usually—that the relevant electronic states are the ones near the Fermi points and their dispersion relation can be approximated by straight lines

with slopes $\pm\hbar v_a$ and $\pm\hbar v_b$ around the Fermi points $\pm k_a$ and $\pm k_b$, respectively. If the lattice constant is taken to be unity

$$\hbar v_{a(b)} = 2t \sin k_{a(b)}, \quad (4)$$

and the value of the Fermi momenta is determined by the overall filling of the band and the splitting of the subbands, $2t_\perp$. It follows from the symmetry of the tight-binding dispersion relation of the free chain that—as shown in Fig. 2—for a half-filled system $v_a = v_b$, while more generally $v_a \neq v_b$.

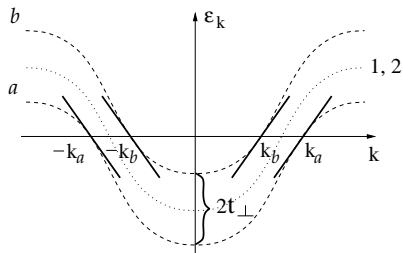


FIG. 2: The linearized spectrum for a half-filled ladder.

Measuring the momenta from the respective Fermi points the kinetic energy takes the form

$$\mathcal{H}_{\text{kin}} = \sum_{k,\sigma} \left[\hbar v_a k (a_{k_a+k,\sigma}^\dagger a_{k_a+k,\sigma} - a_{-k_a+k,\sigma}^\dagger a_{-k_a+k,\sigma}) + \hbar v_b k (b_{k_b+k,\sigma}^\dagger b_{k_b+k,\sigma} - b_{-k_b+k,\sigma}^\dagger b_{-k_b+k,\sigma}) \right]. \quad (5)$$

The operators $a_{\pm k_a+k,\sigma}^\dagger$ ($a_{\pm k_a+k,\sigma}$) and $b_{\pm k_b+k,\sigma}^\dagger$ ($b_{\pm k_b+k,\sigma}$) create (annihilate) an electron with momentum k and spin σ around the Fermi points $\pm k_a$ and $\pm k_b$, respectively. Thus, the linearized spectrum consists of four branches, two corresponding to right-moving particles and two to left movers. In what follows the notation

$$\begin{aligned} a_{+,k,\sigma} &\equiv a_{k_a+k,\sigma}, & a_{-,k,\sigma} &\equiv a_{-k_a+k,\sigma}, \\ b_{+,k,\sigma} &\equiv b_{k_b+k,\sigma}, & b_{-,k,\sigma} &\equiv b_{-k_b+k,\sigma} \end{aligned} \quad (6)$$

will be used.

For simplicity a sharp cut-off is assumed in the allowed momenta, $|k| < k_0$, leading to bandwidths $2E_{a(b)} = 2\hbar v_{a(b)}k_0$, which in general are different. It is also assumed that the bandwidth is comparable or less than the splitting of the bands, in other words the difference $k_a - k_b$ is comparable or larger than the cut-off k_0 . Due to this choice, from the results presented in this paper, it is not possible to recover the limit of uncoupled chains.

B. Interactions

When the on-site Hubbard interaction is written in terms of the operators of right and left-moving fermions

of type a and b , the terms appearing have the generic form

$$\alpha_{\lambda_1,k_1,\sigma}^\dagger \beta_{\lambda_2,k_2,\sigma'}^\dagger \gamma_{\lambda_3,k_3,\sigma'} \delta_{\lambda_4,k_4,\sigma}, \quad (7)$$

where the operators α^\dagger , β^\dagger , γ and δ are creation and annihilation operators of particles of type a or b , and $\lambda_i = \pm$. While in the Hubbard ladder the strength of all these processes is related to the single on-site Coulomb repulsion U , in what follows a more general Hamiltonian will be used allowing for different couplings for the different scattering processes.

The coupling constant of the process given in (7) will be assumed to be momentum independent and will be denoted by

$$g_{\{\lambda_i\},\sigma\sigma'}^{\alpha\beta\gamma\delta}. \quad (8)$$

It is clear that the terms with couplings

$$g_{\lambda_1,\lambda_2,\lambda_3,\lambda_4,\sigma\sigma'}^{\alpha\beta\gamma\delta} \quad \text{and} \quad g_{\lambda_2,\lambda_1,\lambda_4,\lambda_3,\sigma'\sigma}^{\beta\alpha\delta\gamma} \quad (9)$$

describe the same process. Similarly, the terms with couplings

$$g_{\lambda_1,\lambda_2,\lambda_3,\lambda_4,\sigma\sigma'}^{\alpha\beta\gamma\delta} \quad \text{and} \quad g_{\lambda_4,\lambda_3,\lambda_2,\lambda_1,\sigma\sigma'}^{\delta\gamma\beta\alpha} \quad (10)$$

are Hermitian conjugates to each other. Assuming that the couplings are real, the same coupling constant is used for them. If the system has inversion symmetry, the couplings

$$g_{\lambda_1,\lambda_2,\lambda_3,\lambda_4,\sigma\sigma'}^{\alpha\beta\gamma\delta} \quad \text{and} \quad g_{-\lambda_1,-\lambda_2,-\lambda_3,-\lambda_4,\sigma\sigma'}^{\alpha\beta\gamma\delta}, \quad (11)$$

or when combining with (9) the couplings

$$g_{\lambda_1,\lambda_2,\lambda_3,\lambda_4,\sigma\sigma'}^{\alpha\beta\gamma\delta} \quad \text{and} \quad g_{-\lambda_2,-\lambda_1,-\lambda_4,-\lambda_3,\sigma'\sigma}^{\beta\alpha\delta\gamma} \quad (12)$$

should be taken to be identical. Furthermore, since we have taken the symmetric and antisymmetric combinations of the operators belonging to the chains, only such scattering processes survive in which all four particles are in band a or in band b , or two of them are of type a and two of them are of type b .

A scattering process is *intra*band if all participating particles belong to the same subband (a or b), $\alpha = \beta = \gamma = \delta$. The processes in which either $\alpha \neq \beta$ or $\alpha \neq \delta$ are *inter*band. The terms with coupling of type g^{aabb} describe processes in which charge is transferred from one band to the other. If $\sigma \neq \sigma'$ in an interband process with coupling g^{abab} , the scattering is accompanied by a spin flip in the bands. This could be considered as the analogue of the Kondo coupling.

It can be assumed that in a non-polarized system the coupling constants depend on the relative orientation of the spins only. As a further constraint we will distinguish two cases only, whether $\sigma = \sigma'$ or $\sigma \neq \sigma'$. The index \parallel or \perp will be used for them.

Momentum conservation gives two further restrictions:

$$k_1 + k_2 = k_3 + k_4 \quad (13)$$

and

$$\lambda_1 k_\alpha + \lambda_2 k_\beta = \lambda_3 k_\gamma + \lambda_4 k_\delta + G, \quad (14)$$

where G is a reciprocal lattice vector. $G = 0$ corresponds to normal processes, while G is finite for umklapp processes. Since it was assumed that k_a and k_b are sufficiently different, momentum conservation (including umklapp processes) can be satisfied only if:

1. All four particles participating in a scattering process are right movers or all of them are left movers,

$$\lambda_1 = \lambda_2 = \lambda_3 = \lambda_4. \quad (15)$$

Conventionally these processes are labelled by an index 4. They will be neglected since—as opposed to the other processes—their contribution is not logarithmically divergent in perturbation theory. Normally they lead to a Fermi velocity renormalization only.

2. Two right (left) movers are scattered into two left (right) movers,

$$\lambda_1 = \lambda_2 = -\lambda_3 = -\lambda_4. \quad (16)$$

These are the umklapp processes and they will be labelled by an index 3.

3. A right and a left mover scatter on each other and again a right and left mover are created. Depending on whether the momentum transfer between the particles of the same spin is small

$$\lambda_1 = -\lambda_2 = -\lambda_3 = \lambda_4 \quad (17)$$

or large,

$$\lambda_1 = -\lambda_2 = \lambda_3 = -\lambda_4 \quad (18)$$

the processes are labelled by indices 2 or 1.

The momentum transfer is small, the process is forward scattering, if either $k_\alpha - k_\delta = 0$ (and consequently $k_\gamma - k_\beta = 0$) or $k_\alpha - k_\delta = \pm(k_a - k_b)$. As shown in Fig. 3 six such processes are possible.

Besides the intraband processes, either in band a or in band b , there are four possible interband processes. Two particles from band b are scattered into band a , or vice versa, in channels $a^\dagger a^\dagger b b$ and $b^\dagger b^\dagger a a$, and a small momentum of order $\pm(k_a - k_b)$ is transferred between right-moving and left-moving particles, respectively. The transferred momentum can be arbitrary small in the processes $a^\dagger b^\dagger b a$ and $b^\dagger a^\dagger a b$. An $a^\dagger b^\dagger a b$ process with small momentum transfer is possible only when all particles are right or left movers, and these processes—as mentioned above—will be neglected.

Taking into account that the processes $a^\dagger a^\dagger b b$ and $b^\dagger b^\dagger a a$ are Hermitian conjugates and the process $b^\dagger a^\dagger a b$ can be obtained from an $a^\dagger b^\dagger b a$ process by inversion, the

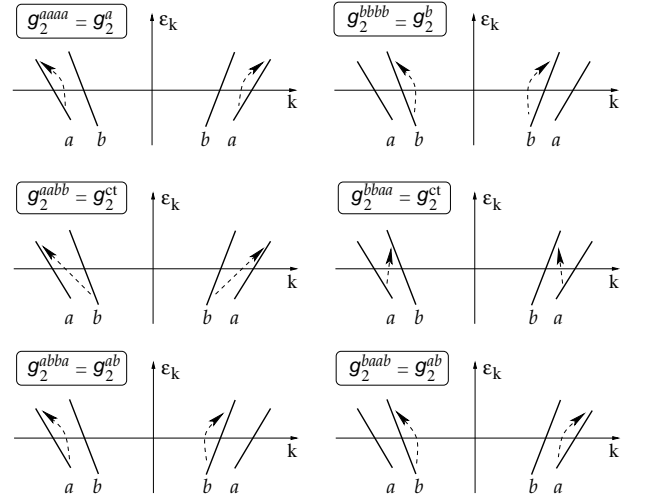


FIG. 3: Forward (g_2) scattering processes in a ladder system.

forward-scattering processes are characterized by 8 coupling constants:

$$\begin{aligned} g_{2\parallel}^a &\equiv g_{2\parallel}^{aaaa}, & g_{2\perp}^a &\equiv g_{2\perp}^{aaaa}, \\ g_{2\parallel}^b &\equiv g_{2\parallel}^{bbbb}, & g_{2\perp}^b &\equiv g_{2\perp}^{bbbb}, \\ g_{2\parallel}^{ab} &\equiv g_{2\parallel}^{abba}, & g_{2\perp}^{ab} &\equiv g_{2\perp}^{abba}, \\ g_{2\parallel}^{ct} &\equiv g_{2\parallel}^{aabb}, & g_{2\perp}^{ct} &\equiv g_{2\perp}^{aabb}. \end{aligned} \quad (19)$$

For six of these eight forward-scattering processes, the particles remain in the same branch of the spectrum. As we will see, they play a special role. Due to the conservation of the number of particles and of the spin in each branch, if they act alone, Luttinger-liquid-like behavior is found.

In the large-momentum-transfer processes, $\lambda_1 = -\lambda_4$ and $\lambda_2 = -\lambda_3$, and consequently $k_\alpha - k_\delta = \pm 2k_a, \pm 2k_b$ or $\pm(k_a + k_b)$, one has to distinguish normal (labelled by 1) and umklapp (labelled by 3) processes. Considering first the normal backward-scattering processes, two of them ($a^\dagger a^\dagger a a$ and $b^\dagger b^\dagger b b$) correspond to intraband processes, and four of them ($a^\dagger a^\dagger b b, b^\dagger b^\dagger a a, a^\dagger b^\dagger a b$, and $b^\dagger a^\dagger b a$) are interband processes. The processes $a^\dagger b^\dagger b a$ and $b^\dagger a^\dagger a b$ are forbidden by momentum conservation for finite hopping amplitude. The six allowed normal backward-scattering processes are shown in Fig. 4.

Since the processes $a^\dagger a^\dagger b b$ and $b^\dagger b^\dagger a a$ are Hermitian conjugates to each other and the processes $a^\dagger b^\dagger a b$ and $b^\dagger a^\dagger b a$ are related by inversion, these processes— analogously to the forward-scattering ones—could be characterized by 8 coupling constants. The backward and forward-scattering terms are, however, not independent when the particles have identical spins. Looking at the terms with couplings $g_{1\parallel}^{abab}$ and $g_{2\parallel}^{abba}$ given by

$$\begin{aligned} \frac{1}{L} \sum_{k, k', q} & (g_{1\parallel}^{abab} a_{+, k+q, \sigma}^\dagger b_{-, k'-q, \sigma}^\dagger a_{+, k', \sigma} b_{-, k, \sigma} \\ & + g_{2\parallel}^{abba} a_{+, k+q, \sigma}^\dagger b_{-, k'-q, \sigma}^\dagger b_{-, k', \sigma} a_{+, k, \sigma}), \end{aligned} \quad (20)$$

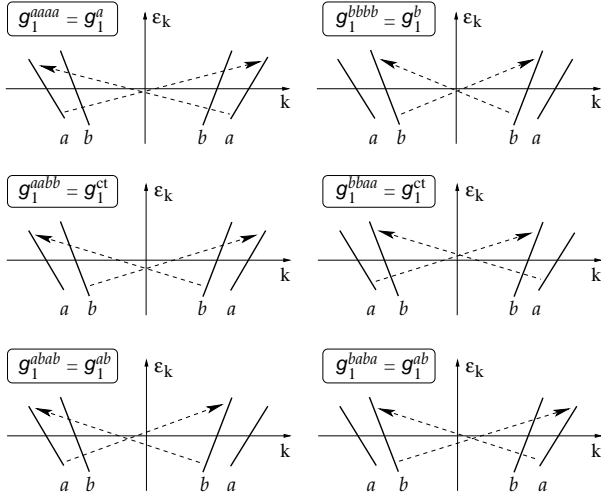


FIG. 4: Backward (g_1) scattering processes in a ladder system.

these are the processes in the last rows of Figs. 3 and 4, it is easily seen that—due to the indistinguishability of the fermions—they describe exactly the same process, if the model is defined by a bandwidth cut-off, as is the case in our model. There is only a sign difference in their contribution. Similar arguments are valid for the couplings $g_{1\parallel}^a$ and $g_{2\parallel}^a$ and also for $g_{1\parallel}^{\text{ct}}$ and $g_{2\parallel}^{\text{ct}}$. For this reason we use the combinations:

$$\begin{aligned} g_{\parallel}^a &\equiv g_{1\parallel}^a - g_{2\parallel}^a, \\ g_{\parallel}^b &\equiv g_{1\parallel}^b - g_{2\parallel}^b, \\ g_{\parallel}^{ab} &\equiv g_{1\parallel}^{ab} - g_{2\parallel}^{ab}, \\ g_{\parallel}^{\text{ct}} &\equiv g_{1\parallel}^{\text{ct}} - g_{2\parallel}^{\text{ct}}, \end{aligned} \quad (21)$$

and only the processes with couplings $g_{1\perp}^a$, $g_{1\perp}^b$, $g_{1\perp}^{ab}$, and $g_{1\perp}^{\text{ct}}$ are true backward-scattering processes.

When either band a , band b or the whole spectrum is half-filled, it is possible that $\lambda_1 k_\alpha + \lambda_2 k_\beta = \lambda_3 k_\gamma + \lambda_4 k_\delta + G$ with a vector of the reciprocal lattice. In the first case intraband umklapp processes are allowed for, while in the second case there are four kinds of interband umklapp processes as shown in Fig. 5, but as mentioned above, two of them appear with the same coupling constant.

Due to the requirement of antisymmetry of the products of fermion operators, no intraband umklapp processes are allowed between particles of the same spin. This is also true for the charge-transfer umklapp processes of type $a_{+\sigma}^\dagger a_{+\sigma}^\dagger b_{-\sigma} b_{-\sigma}$. However, interband umklapp processes of type $a_{+\sigma}^\dagger b_{+\sigma}^\dagger a_{-\sigma} b_{-\sigma}$ and $a_{+\sigma}^\dagger b_{+\sigma}^\dagger b_{-\sigma} a_{-\sigma}$ are not excluded by symmetry. Since they correspond to the same type of process the notation

$$g_{3\parallel}^{ab} \equiv g_{3\parallel}^{abab} - g_{3\parallel}^{abba} \quad (22)$$

will be used. Thus altogether two intraband and four in-

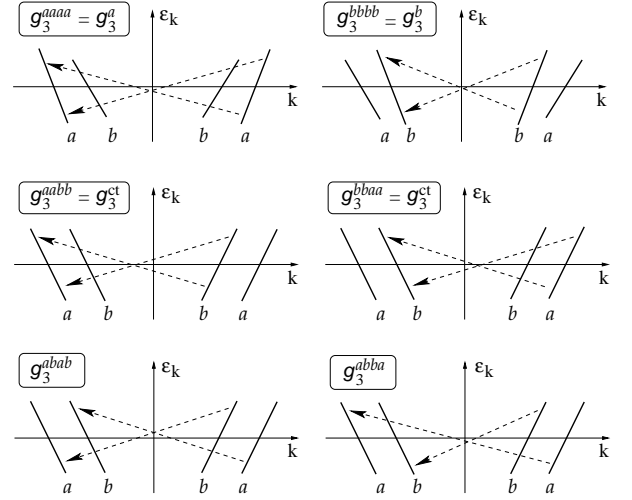


FIG. 5: Umklapp (g_3) processes in a ladder system.

terband umklapp processes with different coupling constants could be distinguished.

In order to get simpler formulas in what follows the dimensionless couplings

$$g_i^{\alpha\beta\gamma\delta} \equiv \frac{g_i^{\alpha\beta\gamma\delta}}{\frac{1}{2}\pi\hbar(v_\alpha + v_\beta + v_\gamma + v_\delta)} \quad (23)$$

and the quantity

$$\gamma = \frac{(v_a + v_b)^2}{4v_a v_b} \quad (24)$$

will be used. γ characterizes the relative slopes of the two bands. $\gamma = 1$ if and only if $v_a = v_b$, while $\gamma > 1$ otherwise, if both v_a and v_b are positive.

III. RENORMALIZATION-GROUP TREATMENT

The perturbative corrections to the vertices and self energy of the 1D interacting fermion system defined by the Hamiltonian in (1) and (2) are logarithmically singular. A convenient procedure to sum up the leading or next-to-leading logarithmic corrections to any order of the couplings is provided by the multiplicative renormalization-group method (for a detailed description see Ref. 28). Although the bandwidth is different in the two bands, in the logarithmic approximation a common cut-off can be used,¹⁶ i.e., in the argument of the logarithm, a quantity ω/E_0 will be used instead of ω/E_a , ω/E_b or $2\omega/(E_a + E_b)$.

Up to second order in the couplings the renormalization-group procedure leads to the following scaling equations (here $x = E'_0/E_0$, and prime denotes the renormalized cut-off): for the forward-scattering terms without charge transfer between the bands

$$\frac{dg_{\parallel}^a}{d \ln x} = (n-1)(g_{1\perp}^a)^2 - \gamma(g_{\parallel}^{\text{ct}})^2 \quad (25a)$$

$$+ (n-1) \left[(g_{3\perp}^{abba})^2 + (g_{3\perp}^a)^2 \right] + (g_{3\parallel}^{ab})^2,$$

$$\frac{dg_{2\perp}^a}{d \ln x} = (g_{1\perp}^a)^2 + \gamma(g_{1\perp}^{\text{ct}})^2 + \gamma(g_{2\perp}^{\text{ct}})^2 - (g_{3\perp}^{abab})^2 - (g_{3\perp}^a)^2, \quad (25b)$$

$$\frac{dg_{\parallel}^b}{d \ln x} = (n-1)(g_{1\perp}^b)^2 - \gamma(g_{\parallel}^{\text{ct}})^2 + (n-1) \left[(g_{3\perp}^{abba})^2 + (g_{3\perp}^b)^2 \right] + (g_{3\parallel}^{ab})^2, \quad (25c)$$

$$\frac{dg_{2\perp}^b}{d \ln x} = (g_{1\perp}^b)^2 + \gamma(g_{1\perp}^{\text{ct}})^2 + \gamma(g_{2\perp}^{\text{ct}})^2 - (g_{3\perp}^{abab})^2 - (g_{3\perp}^b)^2, \quad (25d)$$

$$\frac{dg_{\parallel}^{ab}}{d \ln x} = (g_{\parallel}^{\text{ct}})^2 + (n-1) \left[(g_{1\perp}^{\text{ct}})^2 + (g_{1\perp}^{ab})^2 + (g_{3\perp}^{\text{ct}})^2 + (g_{3\perp}^{abab})^2 \right] + (g_{3\parallel}^{ab})^2, \quad (25e)$$

$$\frac{dg_{2\perp}^{ab}}{d \ln x} = (g_{1\perp}^{ab})^2 - (g_{2\perp}^{\text{ct}})^2 - (g_{3\perp}^{abba})^2 - (g_{3\perp}^{\text{ct}})^2, \quad (25f)$$

for the backward-scattering terms without charge transfer

$$\frac{dg_{1\perp}^a}{d \ln x} = 2g_{1\perp}^a \left[g_{\parallel}^a + g_{2\perp}^a \right] + 2\gamma g_{1\perp}^{\text{ct}} g_{2\perp}^{\text{ct}} - 2g_{3\parallel}^{ab} g_{3\perp}^{abba} + (n-2) \left[(g_{1\perp}^a)^2 + (g_{3\perp}^{abba})^2 + (g_{3\perp}^a)^2 \right], \quad (26a)$$

$$\frac{dg_{1\perp}^b}{d \ln x} = 2g_{1\perp}^b \left[g_{\parallel}^b + g_{2\perp}^b \right] + 2\gamma g_{1\perp}^{\text{ct}} g_{2\perp}^{\text{ct}} - 2g_{3\parallel}^{ab} g_{3\perp}^{abba} + (n-2) \left[(g_{1\perp}^b)^2 + (g_{3\perp}^{abba})^2 + (g_{3\perp}^b)^2 \right], \quad (26b)$$

$$\frac{dg_{1\perp}^{ab}}{d \ln x} = 2g_{1\perp}^{ab} \left[g_{\parallel}^{ab} + g_{2\perp}^{ab} \right] + 2g_{1\perp}^{\text{ct}} g_{\parallel}^{\text{ct}} + 2g_{3\parallel}^{ab} g_{3\perp}^{abab} + (n-2) \left[(g_{1\perp}^{ab})^2 + (g_{1\perp}^{\text{ct}})^2 + (g_{3\perp}^{abab})^2 + (g_{3\perp}^{\text{ct}})^2 \right], \quad (26c)$$

for the charge-transfer terms

$$\frac{dg_{\parallel}^{\text{ct}}}{d \ln x} = -g_{\parallel}^{\text{ct}} \left[g_{\parallel}^a + g_{\parallel}^b - 2g_{\parallel}^{ab} \right] + 2(n-1) \left[g_{1\perp}^{\text{ct}} g_{1\perp}^{ab} + g_{3\perp}^{\text{ct}} g_{3\perp}^{abab} \right], \quad (27a)$$

$$\frac{dg_{2\perp}^{\text{ct}}}{d \ln x} = g_{1\perp}^{\text{ct}} \left[g_{1\perp}^a + g_{1\perp}^b \right] + g_{2\perp}^{\text{ct}} \left[g_{2\perp}^a + g_{2\perp}^b - 2g_{2\perp}^{ab} \right] - 2g_{3\perp}^{\text{ct}} g_{3\perp}^{abba}, \quad (27b)$$

$$\frac{dg_{1\perp}^{\text{ct}}}{d \ln x} = g_{1\perp}^{\text{ct}} \left[g_{2\perp}^a + g_{2\perp}^b + 2g_{\parallel}^{ab} + 2(n-2)g_{1\perp}^{ab} \right] + g_{2\perp}^{\text{ct}} \left[g_{1\perp}^a + g_{1\perp}^b \right] + 2g_{\parallel}^{\text{ct}} g_{1\perp}^{ab} + 2(n-2)g_{3\perp}^{\text{ct}} g_{3\perp}^{abab} + 2g_{3\parallel}^{ab} g_{3\perp}^{\text{ct}}, \quad (27c)$$

for the intraband umklapp processes

$$\frac{dg_{3\perp}^a}{d \ln x} = 2g_{3\perp}^a \left[g_{\parallel}^a + (n-2)g_{1\perp}^a - g_{2\perp}^a \right], \quad (28a)$$

$$\frac{dg_{3\perp}^b}{d \ln x} = 2g_{3\perp}^b \left[g_{\parallel}^b + (n-2)g_{1\perp}^b - g_{2\perp}^b \right], \quad (28b)$$

and for the interband umklapp processes

$$\frac{dg_{3\perp}^{abab}}{d \ln x} = g_{3\perp}^{abab} \left[2g_{\parallel}^{ab} + 2(n-2)g_{1\perp}^{ab} - g_{2\perp}^a - g_{2\perp}^b \right] + 2g_{3\parallel}^{ab} g_{1\perp}^{ab} + 2g_{3\perp}^{\text{ct}} \left[g_{\parallel}^{\text{ct}} + (n-2)g_{1\perp}^{\text{ct}} \right], \quad (29a)$$

$$\frac{dg_{3\perp}^{abba}}{d \ln x} = g_{3\perp}^{abba} \left[g_{\parallel}^a + g_{\parallel}^b - 2g_{2\perp}^{ab} + (n-2)(g_{1\perp}^a + g_{1\perp}^b) \right] - 2g_{3\perp}^{\text{ct}} g_{2\perp}^{\text{ct}} - g_{3\parallel}^{ab} \left[g_{1\perp}^a + g_{1\perp}^b \right], \quad (29b)$$

$$\frac{dg_{3\parallel}^{ab}}{d \ln x} = -(n-1) \left[2g_{3\perp}^{abab} g_{1\perp}^{ab} + 2g_{3\perp}^{\text{ct}} g_{1\perp}^{\text{ct}} \right] - g_{3\parallel}^{ab} \left[2g_{\parallel}^{ab} + g_{\parallel}^a + g_{\parallel}^b \right] + (n-1)g_{3\perp}^{abba} \left[g_{1\perp}^a + g_{1\perp}^b \right], \quad (29c)$$

$$\frac{dg_{3\perp}^{\text{ct}}}{d \ln x} = 2g_{3\perp}^{\text{ct}} \left(g_{\parallel}^{ab} + (n-2)g_{1\perp}^{ab} - g_{2\perp}^{ab} \right) + 2g_{3\perp}^{abab} \left(g_{\parallel}^{\text{ct}} + (n-2)g_{1\perp}^{\text{ct}} \right) - 2g_{3\perp}^{abba} g_{2\perp}^{\text{ct}} + 2g_{3\parallel}^{ab} g_{1\perp}^{\text{ct}}. \quad (29d)$$

These systems of equations are the generalizations of the set of equations investigated in detail in Ref. 16 to n -valued spin and to the case when umklapp processes are taken into account. As it will be discussed, depending on the filling of the bands some or all umklapp processes could be neglected, because momentum conservation cannot be satisfied for states near the Fermi points.

Once the scaling equations have been derived one can look for their fixed points. Two types of fixed points can be distinguished. One of them corresponds to fixed points, where some of the couplings vanish while all others remain weak, the dimensionless couplings introduced

in (23) are less than unity. In what follows the term fixed point is used even if the marginal couplings scale to non-universal values on an extended hypersurface in the space of couplings.

In the other type of fixed points at least some of the couplings scale to large values. Using the scaling equations derived in the leading logarithmic approximation these couplings scale to infinity. When the next-to-leading logarithmic corrections are taken into account, finite strong-coupling fixed points are obtained, but they are located outside the region of validity of the low-order calculation. On the basis of this perturbative approach

one cannot decide whether these couplings scale to a finite fixed point with dimensionless strength larger than unity or to infinity. Fortunately, for the characterization of the phases it is sufficient to know whether these couplings are relevant or irrelevant.

IV. TOMONAGA-LUTTINGER FIXED POINT

In the most general case the model is characterized by 18 coupling constants, six of them belong to forward-scattering processes without charge transfer, three are backward-scattering processes without charge transfer, three correspond to charge-transfer processes and six to umklapp processes. When all true backward-scattering processes are irrelevant, their coupling constants scale to zero,

$$g_{1\perp}^{a*} = g_{1\perp}^{b*} = g_{1\perp}^{ab*} = 0, \quad (30)$$

all processes in which charge is transferred from one band to the other are also irrelevant,

$$g_{\parallel}^{\text{ct}*} = g_{1\perp}^{\text{ct}*} = g_{2\perp}^{\text{ct}*} = 0, \quad (31)$$

and all umklapp processes are irrelevant, the right-hand sides of the scaling equations for the couplings of the forward-scattering processes vanish also. This fixed point will be denoted as FP-TL, referring to the fact that only those processes survive in which charge and spin conservation are satisfied in each branch of the spectrum, and therefore Tomonaga-Luttinger behavior is expected.

A. Stability analysis

The behavior of the couplings close to a fixed point can be studied analytically using the eigenvalues of the linearized matrix

$$L_{ij} = \frac{g'_i}{g_j} \Big|_{\{g^*\}} \quad (32)$$

of the renormalization-group transformation, where prime denotes the renormalized coupling, i and j are short-hand notations for all indices, and $*$ refers to the fixed-point value. Deviations from the fixed-point are relevant if the eigenvalue is larger than unity, they are irrelevant if the eigenvalue is less than unity. A unit eigenvalue indicates marginal direction. Whether a marginal direction is marginally relevant or marginally irrelevant is determined by higher-order corrections.

First the case of generic band filling is studied, when all umklapp processes can be neglected. In the weak-coupling regime near FP-TL the matrix L_{ij} defined in (32) can be diagonalized. The 12 eigenvalues are:

$$\lambda_1 = 1 + 2(g_{\parallel}^{a*} + g_{2\perp}^{a*}) \ln x, \quad (33a)$$

$$\lambda_2 = 1 + 2(g_{\parallel}^{b*} + g_{2\perp}^{b*}) \ln x, \quad (33b)$$

$$\lambda_3 = 1 + 2(g_{\parallel}^{ab*} + g_{2\perp}^{ab*}) \ln x, \quad (33c)$$

$$\lambda_4 = 1 + (-g_{\parallel}^{a*} - g_{\parallel}^{b*} + 2g_{\parallel}^{ab*}) \ln x, \quad (33d)$$

$$\lambda_5 = 1 + (g_{2\perp}^{a*} + g_{2\perp}^{b*} + 2g_{\parallel}^{ab*}) \ln x, \quad (33e)$$

$$\lambda_6 = 1 + (g_{2\perp}^{a*} + g_{2\perp}^{b*} - 2g_{2\perp}^{ab*}) \ln x \quad (33f)$$

and the six other eigenvalues are equal to 1. The fixed point can be attractive if the eigenvalues $\lambda_1, \dots, \lambda_6$ are not greater than unity. Since during the renormalization procedure the cut-off is scaled to smaller values, the logarithmic multiplicative factor has negative sign, the coupling constant combinations appearing in the brackets have to be non-negative in the irrelevant directions. Thus for generic band filling FP-TL can be attractive if the following inequalities hold:

$$g_{\parallel}^{a*} \geq -g_{2\perp}^{a*}, \quad (34a)$$

$$g_{\parallel}^{b*} \geq -g_{2\perp}^{b*}, \quad (34b)$$

$$g_{\parallel}^{ab*} \geq -g_{2\perp}^{ab*}, \quad (34c)$$

$$2g_{\parallel}^{ab*} \geq g_{\parallel}^{a*} + g_{\parallel}^{b*}, \quad (34d)$$

$$2g_{\parallel}^{ab*} \geq -g_{2\perp}^{a*} - g_{2\perp}^{b*}, \quad (34e)$$

$$g_{2\perp}^{a*} + g_{2\perp}^{b*} \geq 2g_{2\perp}^{ab*}. \quad (34f)$$

Although these relations give the stability condition of the fixed point only and cannot be used to get the whole basin of attraction, clearly the Tomonaga-Luttinger fixed point has an extended basin of attraction in the parameter space.

When either band a or band b is half filled, i.e., $4k_a$ or $4k_b$ is equal to a reciprocal lattice vector G , the contributions of the intraband umklapp processes have to be taken into account. We will consider the process $g_{3\perp}^a$ but the results can be easily extended to the case when $g_{3\perp}^b$ is relevant by replacing the couplings g_i^a by the corresponding g_i^b . FP-TL is recovered if besides the requirements given in (30) (backward-scattering processes are irrelevant) and (31) (charge-transfer processes are irrelevant) the intraband umklapp process, too, is irrelevant, the fixed-point value of its coupling vanishes:

$$g_{3\perp}^{a*} = 0. \quad (35)$$

With one new coupling added the 13 eigenvalues of the stability matrix L_{ij} are as follows: 12 of them are the same as given earlier in (33), and the 13th eigenvalue is

$$\lambda_{13} = 1 + 2(g_{\parallel}^{a*} - g_{2\perp}^{a*}) \ln x. \quad (36)$$

The condition of stability of the fixed point is similar to the case discussed above, except that the requirement $g_{\parallel}^{a*} \geq g_{2\perp}^{a*}$ changes the first inequality to

$$g_{\parallel}^{a*} \geq |g_{2\perp}^{a*}|. \quad (37)$$

This means that Luttinger-liquid behavior is expected in a smaller region of the parameter space.

The situation is similar when the system is half-filled, $2(k_a + k_b)$ is equal to a reciprocal lattice vector G and therefore the interband umklapp processes have to be taken into account. In this case the two Fermi velocities are equal ($\gamma = 1$). A weak-coupling FP-TL is obtained if besides the backward-scattering processes (30) and charge-transfer processes (31) all interband umklapp processes are irrelevant,

$$g_{3\perp}^{abab^*} = g_{3\perp}^{abba^*} = g_{3\perp}^{aabb^*} = g_{3\parallel}^{ab^*} = 0. \quad (38)$$

In this case 16 coupling constants have to be taken into account. 12 of the 16 eigenvalues are the same as for generic filling and the remaining 4 are:

$$\lambda_{13} = 1 + 2(g_{\parallel}^{ab^*} - g_{2\perp}^{ab^*}) \ln x, \quad (39a)$$

$$\lambda_{14} = 1 + (-g_{2\perp}^{a^*} - g_{2\perp}^{b^*} + 2g_{\parallel}^{ab^*}) \ln x, \quad (39b)$$

$$\lambda_{15} = 1 + (g_{\parallel}^{a^*} + g_{\parallel}^{b^*} - 2g_{2\perp}^{ab^*}) \ln x, \quad (39c)$$

$$\lambda_{16} = 1 + (-g_{\parallel}^{a^*} - g_{\parallel}^{b^*} + 2g_{\parallel}^{ab^*}) \ln x, \quad (39d)$$

The attractive region of the weak-coupling fixed point is determined by the inequalities:

$$g_{\parallel}^{a^*} \geq -g_{2\perp}^{a^*}, \quad (40a)$$

$$g_{\parallel}^{b^*} \geq -g_{2\perp}^{b^*}, \quad (40b)$$

$$g_{\parallel}^{ab^*} \geq |g_{2\perp}^{ab^*}|, \quad (40c)$$

$$2g_{\parallel}^{ab^*} \geq g_{\parallel}^{a^*} + g_{\parallel}^{b^*}, \quad (40d)$$

$$2g_{\parallel}^{ab^*} \geq |g_{2\perp}^{a^*} + g_{2\perp}^{b^*}|, \quad (40e)$$

$$g_{2\perp}^{a^*} + g_{2\perp}^{b^*} \geq 2g_{2\perp}^{ab^*}, \quad (40f)$$

$$g_{\parallel}^{a^*} + g_{\parallel}^{b^*} \geq 2g_{2\perp}^{ab^*} \quad (40g)$$

The basin of attraction of the Tomonaga-Luttinger fixed point is further reduced by the requirement that all interband umklapp processes should be irrelevant.

One can see that FP-TL cannot be reached when the model is fully attractive, when the initial values of all couplings are negative. On the other hand in a fully repulsive model, when the initial values of all couplings are positive, Luttinger-liquid behavior is a possibility. Unfortunately, as will be seen, the repulsive Hubbard ladder does not belong to this class.

B. Bosonization of the Tomonaga-Luttinger part of the model

It is expected that for such couplings which scale to the weak-coupling FP-TL, this n -component fermionic ladder has $2n$ gapless bosonic excitations, two soft charge and $2(n-1)$ soft spin modes, and therefore the model is equivalent to a $2n$ -component Luttinger liquid. This is shown here by transforming the fixed-point Hamiltonian into bosonic language. For this a more general model will be considered where only intraband and interband forward-scattering terms are allowed without

charge transfer, but the couplings $g_{2;\sigma\sigma'}^a$, $g_{2;\sigma\sigma'}^b$, and $g_{2;\sigma\sigma'}^{ab}$ may depend on σ and σ' separately. It is assumed, however, that they are symmetric in the spin indices,

$$g_{2;\sigma\sigma'}^{a(b,ab)} = g_{2;\sigma'\sigma}^{a(b,ab)}. \quad (41)$$

Introducing the density operators corresponding to particle-hole excitations with small momentum,

$$n_{\pm,\sigma}^a(q) = \sum_k a_{\pm,k,\sigma}^\dagger a_{\pm,k+q,\sigma}, \quad (42)$$

$$n_{\pm,\sigma}^b(q) = \sum_k b_{\pm,k,\sigma}^\dagger b_{\pm,k+q,\sigma},$$

the kinetic energy of the particles in the two bands given in (5) can be written as usual in the form

$$\mathcal{H}_{\text{kin}} = \pi\hbar \sum_{\lambda,\sigma} \int dx \left[v_a (n_{\lambda,\sigma}^a(x))^2 + v_b (n_{\lambda,\sigma}^b(x))^2 \right], \quad (43)$$

where $\lambda = \pm$ and the operators $n_{\lambda,\sigma}^{a(b)}(x)$ are the densities in real space, the Fourier transforms of $n_{\lambda,\sigma}^{a(b)}(q)$. The low-energy part of the spectrum contains excitations with large momentum, too. They correspond to excitations in which the number of particles with a given spin index in a given branch changes. They can be taken into account by giving the change in the number of particles in the branches. For simplicity we will not write out these terms since they do not influence the results.

The interaction terms containing intraband and interband forward-scattering processes without charge transfer can also be expressed in terms of the small-momentum components of the densities:

$$\begin{aligned} \mathcal{H}_{\text{int}}^{\text{Lutt}} = \frac{2\pi\hbar}{L} \sum_{\sigma\sigma'} \sum_q & \left[v_a g_{2;\sigma\sigma'}^a n_{+,\sigma}^a(q) n_{-,\sigma'}^a(-q) \right. \\ & + v_b g_{2;\sigma\sigma'}^b n_{+,\sigma}^b(q) n_{-,\sigma'}^b(-q) \\ & + \frac{1}{4}(v_a + v_b) g_{2;\sigma\sigma'}^{ab} n_{+,\sigma}^a(q) n_{-,\sigma'}^b(-q) \\ & \left. + \frac{1}{4}(v_a + v_b) g_{2;\sigma\sigma'}^{ab} n_{+,\sigma}^b(q) n_{-,\sigma'}^a(-q) \right], \end{aligned} \quad (44)$$

which can be written in real-space representation as

$$\begin{aligned} \mathcal{H}_{\text{int}}^{\text{Lutt}} = 2\pi\hbar \sum_{\sigma\sigma'} \int dx & \left[v_a g_{2;\sigma\sigma'}^a n_{+,\sigma}^a(x) n_{-,\sigma'}^a(x) \right. \\ & + v_b g_{2;\sigma\sigma'}^b n_{+,\sigma}^b(x) n_{-,\sigma'}^b(x) \\ & + \frac{1}{4}(v_a + v_b) g_{2;\sigma\sigma'}^{ab} n_{+,\sigma}^a(x) n_{-,\sigma'}^b(x) \\ & \left. + \frac{1}{4}(v_a + v_b) g_{2;\sigma\sigma'}^{ab} n_{+,\sigma}^b(x) n_{-,\sigma'}^a(x) \right]. \end{aligned} \quad (45)$$

First, the Hamiltonian is diagonalized in its spin indices σ and σ' . To this end we perform an orthogonal transformation to a new basis corresponding to such combinations of the bosonic densities, that two of them (one for each band) are symmetric and $2(n-1)$ ($n-1$ for each band) are antisymmetric in the spin quantum numbers:

$$n_{\lambda,c}^{a(b)}(x) = \frac{1}{\sqrt{n}} \sum_{\sigma=1}^n n_{\lambda,\sigma}^{a(b)}(x), \quad (46)$$

$$n_{\lambda,ms}^{a(b)}(x) = \frac{1}{\sqrt{m(m+1)}} \left(\sum_{\sigma=1}^m n_{\lambda,\sigma}^{a(b)}(x) - mn_{\lambda,m+1}^{a(b)}(x) \right),$$

where $m = 1, \dots, n-1$. This transformation leads to a Hamiltonian in which the spin and charge degrees of freedom are separated,

$$\mathcal{H} = \sum_j \int dx (\mathcal{H}_{\text{kin},j}(x) + \mathcal{H}_{\text{int},j}(x)), \quad (47)$$

where $j = c, 1s, 2s, \dots, (n-1)s$, and the kinetic energy part of the Hamiltonian density is

$$\mathcal{H}_{\text{kin},j}(x) = \pi\hbar \sum_{\lambda} \left[v_a (n_{\lambda,j}^a(x))^2 + v_b (n_{\lambda,j}^b(x))^2 \right], \quad (48)$$

while the interaction term can be written as

$$\begin{aligned} \mathcal{H}_{\text{int},j}(x) = & 2\pi\hbar \left(v_a g_{2;j}^a n_{+,j}^a(x) n_{-,j}^a(x) \right. \\ & + v_b g_{2;j}^b n_{+,j}^b(x) n_{-,j}^b(x) \\ & + \frac{1}{4} g_{2;j}^{ab} (v_a + v_b) n_{+,j}^a(x) n_{-,j}^b(x) \\ & \left. + \frac{1}{4} g_{2;j}^{ab} (v_a + v_b) n_{+,j}^b(x) n_{-,j}^a(x) \right), \end{aligned} \quad (49)$$

and the corresponding couplings are

$$\begin{aligned} g_{2;c}^{a(b,ab)} &= \frac{1}{n} \sum_{\sigma\sigma'=1}^n g_{2;\sigma\sigma'}^{a(b,ab)}, \quad (50) \\ g_{2;ms}^{a(b,ab)} &= \frac{1}{m(m+1)} \sum_{\sigma\sigma'=1}^m g_{2;\sigma\sigma'}^{a(b,ab)} + \frac{m}{m+1} g_{2;m+1,m+1}^{a(b,ab)} \\ &\quad - \frac{1}{m+1} \sum_{\sigma=1}^m \left(g_{2;\sigma,m+1}^{a(b,ab)} + g_{2;m+1,\sigma}^{a(b,ab)} \right). \end{aligned}$$

In order to obtain the velocities of the different modes the Hamiltonian is rewritten in terms of continuum bosonic fields. The fields $\phi_{\lambda,j}^{a(b)}(x)$ are related to the densities by the relation

$$\pi n_{\lambda,j}^{a(b)}(x) = -\partial_x \phi_{\lambda,j}^{a(b)}(x). \quad (51)$$

The total phase fields and their duals are

$$\begin{aligned} \phi_j^{a(b)}(x) &= \phi_{+,j}^{a(b)}(x) + \phi_{-,j}^{a(b)}(x), \\ \theta_j^{a(b)}(x) &= \phi_{+,j}^{a(b)}(x) - \phi_{-,j}^{a(b)}(x). \end{aligned} \quad (52)$$

The fields $\Pi_j^{a(b)}$ defined by

$$\pi \Pi_j^{a(b)}(x) = -\partial_x \theta_j^{a(b)}(x) \quad (53)$$

are canonical conjugates to the fields $\phi_j^{a(b)}(x)$, they satisfy the commutation relation:

$$[\Pi_j^{a(b)}(x), \phi_{j'}^{a(b)}(x')] = i\delta_{jj'} \delta(x-x'). \quad (54)$$

In this representation, the Hamiltonian can be written as

$$\mathcal{H} = \sum_j \int dx (\mathcal{H}_j^a(x) + \mathcal{H}_j^b(x) + \mathcal{H}_j^{ab}(x)), \quad (55)$$

where

$$\mathcal{H}_j^a(x) = \frac{\hbar u_{a,j}}{2\pi} \left[\pi^2 K_{a,j} (\Pi_j^a(x))^2 + \frac{1}{K_{a,j}} (\partial_x \phi_j^a(x))^2 \right], \quad (56)$$

with

$$\begin{aligned} u_{a,j} &= v_a \sqrt{1 - (g_{2;j}^a)^2}, \\ K_{a,j} &= \sqrt{\frac{1 - g_{2;j}^a}{1 + g_{2;j}^a}}, \end{aligned} \quad (57)$$

and similar expressions with index b , and the coupling between the bands is given by

$$\begin{aligned} \mathcal{H}_j^{ab}(x) = & \frac{\hbar(v_a + v_b)}{4\pi} g_{2;j}^{ab} \left[\partial_x \phi_j^a(x) \partial_x \phi_j^b(x) \right. \\ & \left. - \pi^2 \Pi_j^a(x) \Pi_j^b(x) \right]. \end{aligned} \quad (58)$$

The first two terms of the Hamiltonian can be interpreted as the Hamiltonian of two n -component Luttinger liquids. The coupling $\mathcal{H}_j^{ab}(x)$ is diagonal in the component index, it couples the $2n$ components into n pairs. Without this coupling, in the most general case, the $2n$ modes have different velocities, so not only spin-charge separation occurs in the system but all modes appear separately. In the special case, when the couplings depend only on whether $\sigma = \sigma'$ or $\sigma \neq \sigma'$, the couplings are

$$g_{2;c}^{a(b)} = g_{2\parallel}^{a(b)} + (n-1)g_{2\perp}^{a(b)}, \quad (59)$$

and

$$g_{2;ms}^{a(b)} = g_{2\parallel}^{a(b)} - g_{2\perp}^{a(b)}, \quad m = 1, 2, \dots, (n-1), \quad (60)$$

so the $n-1$ spin modes in band a (b) have the same velocity.

The full Hamiltonian can be diagonalized by the ‘‘symmetric’’ and ‘‘antisymmetric’’ combinations of the operators belonging to the two bands:

$$\tilde{\phi}_j^{\pm} = \frac{1}{\sqrt{u_{a,j} + u_{b,j}}} \left[\phi_j^a \sqrt{u_{a,j}/K_{a,j}} \pm \phi_j^b \sqrt{u_{b,j}/K_{b,j}} \right], \quad (61)$$

and similar expression holds for the conjugated momenta:

$$\tilde{\Pi}_j^{\pm} = \frac{1}{\sqrt{u_{a,j} + u_{b,j}}} \left[\Pi_j^a \sqrt{u_{a,j}K_{a,j}} \pm \Pi_j^b \sqrt{u_{b,j}K_{b,j}} \right], \quad (62)$$

such that they satisfy the canonical commutation relation.

With these operators the Hamiltonian density is the sum of $2n$ Tomonaga-Luttinger Hamiltonians:

$$\mathcal{H}(x) = \sum_j (\mathcal{H}_j^+(x) + \mathcal{H}_j^-(x)) \quad (63)$$

where

$$\mathcal{H}_j^\pm(x) = \frac{\hbar\tilde{u}_{\pm,j}}{2\pi} \left[\pi^2 \tilde{K}_{\pm,j} (\tilde{\Pi}_j^\pm(x))^2 + \frac{1}{\tilde{K}_{\pm,j}} (\partial_x \tilde{\phi}_j^\pm(x))^2 \right], \quad (64)$$

and the velocities and Luttinger parameters are given by

$$\begin{aligned} \tilde{u}_{+,j} &= \tilde{u}_{-,j} = (u_{a,j} + u_{b,j}) \sqrt{1 - \tilde{g}_j}, \\ \tilde{K}_{+,j} &= 1/\tilde{K}_{-,j} = \sqrt{\frac{1 + \tilde{g}_j}{1 - \tilde{g}_j}}, \end{aligned} \quad (65)$$

where

$$\tilde{g}_j = \frac{g_{2,j}^{ab}(v_a + v_b)}{2\sqrt{u_{a,j}u_{b,j}/(K_{a,j}K_{b,j})}} \quad (66)$$

The velocities are the same in the two sectors, therefore, in the most general case only n different velocities are found for the $2n$ modes. If the couplings depend on the relative spins of the scattered electrons only, 2 different velocities are found and one recovers the usual spin-charge separation.

V. STRONG-COUPPLING FIXED POINTS

In all other solutions of the scaling equations, some of the backward-scattering, charge-transfer or umklapp processes are relevant and scale to a strong-coupling fixed point. Although these processes may drive the marginal forward-scattering processes, too, to the strong-coupling limit, these fixed points will be classified by giving those backward-scattering, charge-transfer and umklapp processes only, which become relevant.

A. Fixed points

First the backward-scattering terms are considered. It is easy to check that the scaling equations can be satisfied if the charge-transfer and umklapp processes are still irrelevant, they scale to zero, and only some of the backward-scattering processes—together with some forward-scattering ones—scale to strong coupling. FP-BS-a(b) denotes the fixed point where the coupling of the intraband backward scattering in band a (or in band b) has non-vanishing value. The fixed point FP-BS-ab corresponds to the case when the interband backward scattering is relevant and the intraband backscatterings are irrelevant. It is possible that one or both of the intraband and the interband backward-scattering processes

are relevant at the same time, but as we will see these fixed points do not give a new phase.

Similarly, it can be checked that the scaling equations can be satisfied by assuming that in the fixed point, one of the charge-transfer forward-scattering processes has non-vanishing coupling, while all backward-scattering and umklapp processes are irrelevant. Accordingly FP-CT-FS \parallel and FP-CT-FS \perp denote the fixed points where $g_{\parallel}^{\text{ct}}$ or g_{\perp}^{ct} , respectively are relevant, while the other charge-transfer processes are irrelevant.

While the backward-scattering and charge-transfer forward-scattering processes may become relevant on their own, this is not the case for the charge-transfer backward-scattering process $g_{1\perp}^{\text{ct}}$, except if $n = 2$. For $n > 2$, if the charge-transfer backward-scattering process is relevant, it will necessarily drive the interband backscattering processes ($g_{1\perp}^{ab}$) and the charge-transfer processes between electrons of parallel spin ($g_{\parallel}^{\text{ct}}$), too, to strong coupling. The corresponding fixed point is denoted by FP-CT-BS.

Similar situation occurs when one of the bands is half-filled. In this case the intraband umklapp processes may become relevant, and, if $n > 2$ these processes drive the intraband backward-scattering processes, too, to strong coupling. This fixed point is denoted by FP-U-a(b).

The names of the fixed points FP-U-abab, FP-U-abba, FP-U-ab \parallel , and FP-CT-U, which may be reached when the system is half filled, are self-explanatory. E.g., in the fixed point FP-U-abab, the coupling $g_{3\perp}^{abab}$ scales to strong coupling, while in the fixed point FP-U-abba the coupling $g_{3\perp}^{abba}$ is relevant. For $n = 2$, these fixed points can be reached without driving charge-transfer, backward-scattering or other umklapp processes to strong coupling. For $n > 2$, however, necessarily some other couplings are also relevant. E.g., the coupling $g_{3\perp}^{abab}$ will drive the couplings $g_{1\perp}^{ab}$ and $g_{3\parallel}^{ab}$ to strong coupling, or together with $g_{3\perp}^{abba}$ both the intraband backscattering and the umklapp process $g_{3\parallel}^{ab}$ become relevant. The charge-transfer umklapp process drives the interband backward-scattering processes to the strong-coupling limit.

Depending on the band filling other, more complicated fixed points may also be reached if appropriate initial couplings are chosen. They correspond to regions where several of the backward, charge-transfer or umklapp processes become relevant at the same time, although they are not necessarily driven to strong coupling by the other relevant processes.

B. The role of the individual terms

As we have seen the two-leg fermion ladder with n -valued spin has two charge modes and $2(n - 1)$ spin modes. In the strong-coupling fixed points, where one or more backward-scattering, charge-transfer or umklapp processes are relevant, gap may be opened in the spec-

trum of some of the modes. The bosonization procedure allows us to determine how many of the modes are gapped and how many remain gapless. For this we re-express the one-particle fermion fields and the relevant scattering processes in terms of the boson degrees of freedom.

The continuum fermion fields of the right and left moving particles are defined by

$$\begin{aligned} a_{+,k,\sigma} &= \frac{1}{\sqrt{L}} \int \psi_{+,\sigma}^a(x) e^{-i(k_a+k)x} dx, \\ a_{-,k,\sigma} &= \frac{1}{\sqrt{L}} \int \psi_{-,\sigma}^a(x) e^{-i(-k_a+k)x} dx, \end{aligned} \quad (67)$$

and by similar formulas for the operators b which annihilate left or right moving particles in band b . The bosonic phase fields are related to the fermionic fields by the relations

$$\begin{aligned} \psi_{+,\sigma}^{a(b)}(x) &= \frac{1}{2\pi} F_{+,\sigma}^{a(b)} : e^{i\sqrt{4\pi}\phi_{+,\sigma}^{a(b)}(x)} :, \\ \psi_{-,\sigma}^{a(b)}(x) &= \frac{1}{2\pi} F_{-,\sigma}^{a(b)} : e^{i\sqrt{4\pi}\phi_{-,\sigma}^{a(b)}(x)} :. \end{aligned} \quad (68)$$

Here $F_{\pm,\sigma}^{a(b)}$ are the Klein factors which make sure that the fermion operators satisfy the proper anticommutation relations even though the phase fields $\phi_{\pm,\sigma}^{a(b)}$ satisfy bosonic commutation relations and they commute with the Klein factors. The total bosonic fields and their duals are:

$$\begin{aligned} \phi_{\sigma}^{a(b)} &= \phi_{+,\sigma}^{a(b)} + \phi_{-,\sigma}^{a(b)}, \\ \theta_{\sigma}^{a(b)} &= \phi_{+,\sigma}^{a(b)} - \phi_{-,\sigma}^{a(b)}. \end{aligned} \quad (69)$$

These fields are related to the charge and spin fields defined earlier by the relations

$$\begin{aligned} \phi_c^{a(b)} &= \frac{1}{\sqrt{n}} \sum_{\sigma=1}^n \phi_{\sigma}^{a(b)}, \\ \phi_{ms}^{a(b)} &= \frac{1}{\sqrt{m(m+1)}} \left(\sum_{\sigma=1}^m \phi_{\sigma}^{a(b)} - m\phi_{m+1}^{a(b)} \right), \end{aligned} \quad (70)$$

with $m = 1, \dots, n-1$.

In order to see what the role of those scattering processes is which should vanish in the Tomonaga-Luttinger fixed point and which may drive the system into a strong-coupling fixed point, we rewrite them in this continuum boson representation. The true backward-scattering processes are proportional to

$$\begin{aligned} g_{1\perp}^a &\int \left[\sum_{\sigma \neq \sigma'} \cos(\sqrt{4\pi}(\phi_{\sigma}^a - \phi_{\sigma'}^a)) \right] dx, \\ g_{1\perp}^b &\int \left[\sum_{\sigma \neq \sigma'} \cos(\sqrt{4\pi}(\phi_{\sigma}^b - \phi_{\sigma'}^b)) \right] dx, \\ g_{1\perp}^{ab} &\int \left[\sum_{\sigma \neq \sigma'} \cos(\sqrt{\pi}(\phi_{\sigma}^a - \phi_{\sigma'}^a + \phi_{\sigma}^b - \phi_{\sigma'}^b)) \right. \\ &\quad \left. \times \cos(\sqrt{\pi}(\theta_{\sigma}^a - \theta_{\sigma'}^a - \theta_{\sigma}^b + \theta_{\sigma'}^b)) \right] dx. \end{aligned} \quad (71)$$

It follows from the sine-Gordon form of the interactions that they may give rise to gapped soliton solutions either in the charge or spin sector. It is easy to see that the backward-scattering terms contain spin modes only. For this one has to realize that the combinations $\phi_{\sigma}^{a(b)} - \phi_{\sigma'}^{a(b)}$ (and the similar combinations of the dual fields) occurring in the cosine functions are orthogonal to the charge modes $\phi_c^{a(b)}$ ($\theta_c^{a(b)}$). The intraband backward-scattering process opens $n-1$ spin gaps while the interband process ($g_{1\perp}^{ab}$) opens $2(n-1)$ spin gaps.

In boson representation, except for a factor, the charge-transfer processes have the form

$$\begin{aligned} g_{\parallel}^{\text{ct}} &\int \left[\sum_{\sigma} \cos(\sqrt{4\pi}(\theta_{\sigma}^a - \theta_{\sigma}^b)) \right] dx, \\ g_{2\perp}^{\text{ct}} &\int \left[\sum_{\sigma \neq \sigma'} \cos(\sqrt{\pi}(\theta_{\sigma}^a + \theta_{\sigma'}^a - \theta_{\sigma}^b - \theta_{\sigma'}^b)) \right. \\ &\quad \left. \times \cos(\sqrt{\pi}(\phi_{\sigma}^a - \phi_{\sigma'}^a - \phi_{\sigma}^b + \phi_{\sigma'}^b)) \right] dx, \\ g_{1\perp}^{\text{ct}} &\int \left[\sum_{\sigma \neq \sigma'} \cos(\sqrt{\pi}(\theta_{\sigma}^a + \theta_{\sigma'}^a - \theta_{\sigma}^b - \theta_{\sigma'}^b)) \right. \\ &\quad \left. \times \cos(\sqrt{\pi}(\phi_{\sigma}^a - \phi_{\sigma'}^a + \phi_{\sigma}^b - \phi_{\sigma'}^b)) \right] dx. \end{aligned} \quad (72)$$

The first two expressions which describe charge-transfer forward-scattering processes, contain one charge mode and $n-1$ spin modes, moreover, they couple the same modes, and therefore they modify the spectrum in the same way. For this reason we will not distinguish between these processes and the notation FP-CT-FS will be used for any of the two strong-coupling fixed points FS-CT-FS \parallel and FS-CT-FS \perp or for the fixed hypersurface FP-[CT-FS \parallel]+[CT-FS \perp] on which both $g_{\parallel}^{\text{ct}}$ and $g_{2\perp}^{\text{ct}}$ are relevant. In the expression for the charge-transfer backward-processes the first cosine function contains one charge mode and $n-1$ spin modes if $n > 2$, while if $n = 2$ it contains only a charge mode. The second cosine function contains the other $n-1$ spin modes. As a result one charge mode and one spin mode appears in the $g_{1\perp}^{\text{ct}}$ term if $n = 2$, but one charge and $2(n-1)$ spin modes for $n > 2$.

The umklapp terms may also be responsible for the opening of a gap in the excitation spectrum. The intraband umklapp processes have the form:

$$\begin{aligned} g_{3\perp}^a &\int \left[\sum_{\sigma \neq \sigma'} \cos(\sqrt{4\pi}(\phi_{\sigma}^a + \phi_{\sigma'}^a)) \right] dx, \\ g_{3\perp}^b &\int \left[\sum_{\sigma \neq \sigma'} \cos(\sqrt{4\pi}(\phi_{\sigma}^b + \phi_{\sigma'}^b)) \right] dx. \end{aligned} \quad (73)$$

These umklapp processes do not contain spin modes but one charge modes only if $n = 2$, while if $n > 2$ the charge mode is coupled to $n-1$ spin modes.

The interband umklapp processes take the form

$$\begin{aligned}
& g_{3\perp}^{abab} \int \left[\sum_{\sigma \neq \sigma'} \cos(\sqrt{\pi}(\theta_{\sigma}^a - \theta_{\sigma'}^a - \theta_{\sigma}^b + \theta_{\sigma'}^b)) \right. \\
& \quad \left. \times \cos(\sqrt{\pi}(\phi_{\sigma}^a + \phi_{\sigma'}^a + \phi_{\sigma}^b + \phi_{\sigma'}^b)) \right] dx, \\
& g_{3\perp}^{abba} \int \left[\sum_{\sigma \neq \sigma'} \cos(\sqrt{4\pi}(\phi_{\sigma}^a + \phi_{\sigma'}^b)) \right] dx, \\
& g_{3\parallel}^{ab} \int \left[\sum_{\sigma} \cos(\sqrt{4\pi}(\phi_{\sigma}^a + \phi_{\sigma}^b)) \right] dx, \\
& g_{3\perp}^{\text{ct}} \int \left[\sum_{\sigma \neq \sigma'} \cos(\sqrt{\pi}(\phi_{\sigma}^a + \phi_{\sigma'}^a + \phi_{\sigma}^b + \phi_{\sigma'}^b)) \right. \\
& \quad \left. \times \cos(\sqrt{\pi}(\theta_{\sigma}^a + \theta_{\sigma'}^a - \theta_{\sigma}^b - \theta_{\sigma'}^b)) \right] dx.
\end{aligned} \tag{74}$$

The interband umklapp scattering $g_{3\parallel}^{ab}$ involves one charge and $n - 1$ spin modes for any n . For the other terms different behavior is found for $n = 2$ and $n > 2$. The processes $g_{3\perp}^{abab}$ and $g_{3\perp}^{abba}$ involve the same modes, namely they open one charge gap and $2(n - 1)$ spin gaps for $n > 2$, however, only one charge gap and one spin gap are opened if $n = 2$. Therefore similarly to the charge-transfer forward scatterings they (alone or together) produce the same gap structure in the spectrum. In what follows these processes will not be distinguished and the notation FP-U-ab \perp will be used for any of the fixed points FP-U-abab and FP-U-abba or for the hypersurface on which $g_{3\perp}^{abab}$ and $g_{3\perp}^{abba}$ are relevant simultaneously (FP-[U-abab]+[U-abba]).

The term corresponding to charge-transfer umklapp processes contains only two charge modes if $n = 2$, but two charge and $2(n - 1)$ spin modes when $n > 2$, i.e., all modes are gapped.

C. Possible phases

Following Balents and Fisher¹² the phases belonging to the various fixed points will be characterized by the number of gapless charge and spin modes, respectively.

In the attractive regime of the Tomonaga-Luttinger fixed point where all backward-scattering, charge-transfer, and umklapp processes are irrelevant, their couplings scale to zero, both charge modes and all spin modes are gapless. In this C2S2($n - 1$) phase the system is a $2n$ -component Luttinger liquid.

As it has been pointed out earlier, the backward-scattering processes are responsible for opening gaps in the spin sector, while the charge-transfer and umklapp processes may open gaps both in the charge and spin sectors. Because of the special behavior for $n = 2$ this case will be discussed separately.

For generic filling and for $n > 2$ the charge sector remains gapless if the charge-transfer processes are irrelevant. Depending on whether one of the intraband or

the interband backward-scattering processes is relevant, and the fixed point FS-BS-a(b) or FS-BS-ab is reached, a phase C2S($n - 1$) or C2S0 is found, as shown in Table I. Since all spin modes are gapped if the interband backward-scattering is relevant, the gap structure is not modified by the intraband backward-scattering processes. The same phase is obtained irrespective whether these processes are relevant or not. Similarly, because the two intraband backward-scattering terms open gaps in different spin modes, the spin sector is fully gapped when both of them are relevant. The phase is not modified by a relevant or irrelevant interband backward scattering.

fixed point	phase
FP-TL	C2S2($n - 1$)
FP-BS-a(b)	C2S($n - 1$)
FP-[BS-a]+[BS-b] FP-BS-ab	C2S0
FP-CT-FS	C1S($n - 1$)
FP-CT-BS FP-[CT-FS]+[BS-a(b,ab)]	C1S0

TABLE I: Possible fixed points and phases of the n -component fermion ladder for $n > 2$ at generic filling.

The phase realised in the regime where the charge-transfer forward-scattering processes are relevant, can be described as C1S($n - 1$). Finally if both the backward-scattering and charge-transfer processes are relevant, the spin sector is fully gapped and only one charge mode is gapless (C1S0). Due to the fully gapped spin sector in the fixed point FP-CT-BS ($g_{1\perp}^{\text{ct}}$ is relevant), the same phase is obtained for $n > 2$ even if the other backward-scattering processes become relevant.

As we see there is always at least one gapless charge mode, and a gapped charge mode necessarily implies that some of the spin modes become gapped.

The situation is similar for $n = 2$, except that if the charge-transfer backward-scattering processes are relevant, they lead to phase C1S1. However, if either the charge-transfer backward and forward-scattering processes are relevant simultaneously (in this case the couplings related to other backward-scattering processes may be relevant or irrelevant) or the charge-transfer backward-scatterings and at least one of the other backward-scatterings are relevant simultaneously, the whole spin sector is gapped. The phases corresponding to the various fixed points are given in Table II.

When one of the subbands is half filled, and the corresponding intraband umklapp processes are relevant, the coupling $g_{3\perp}^a$ (or $g_{3\perp}^b$) opens one charge gap and $n - 1$ spin gaps. If the backward-scattering processes become relevant simultaneously, they open gaps in the remaining gapless spin modes, while charge-transfer together with the umklapp processes opens gaps in all branches of the spectrum. This, of course, is not modified if besides the umklapp and charge-transfer processes other couplings, e.g., backward scatterings become relevant. The possible phases are given in Table III.

fixed point	phase
FP-TL	C2S2
FP-BS-a(b)	C2S1
FP-[BS-a]+[BS-b] FP-BS-ab	C2S0
FP-CT-BS FP-CT-FS	C1S1
FP-[CT-BS]+[BS-a(b,ab)] FP-[CT-BS]+[CT-FS] FP-[CT-FS]+[BS-a(b,ab)]	C1S0

TABLE II: Possible fixed points and phases of the n -component fermion ladder for $n = 2$ at generic filling.

fixed point	phase
FP-TL	C2S2($n - 1$)
FP-U-a	C1S($n - 1$)
FP-[U-a]+[BS-b(ab)]	C1S0
FP-[U-a]+[CT-BS] FP-[U-a]+[CT-FS]	C0S0

TABLE III: Possible fixed points and phases of the n -component fermion ladder with half-filled subband for $n > 2$.

The phases obtained for $n = 2$ are given in Table IV. The difference compared to $n > 2$ is due to the fact that the intraband umklapp processes open gap in the charge sector only and therefore phases with a fully gapless spin sector and one soft charge mode (C1S2) and a fully gapped charge sector with one soft spin mode (C0S1) are also possible. Similarly to the $n > 2$ case only one charge gap can be found in the spectrum if the charge-transfer processes are irrelevant (phases C1S1 and C1S0).

fixed point	phase
FP-TL	C2S2
FP-U-a	C1S2
FP-[U-a]+[BS-a(b)]	C1S1
FP-[U-a]+[BS-a]+[BS-b] FP-[U-a]+[BS-ab]	C1S0
FP-[U-a]+[CT-BS] FP-[U-a]+[CT-FS]	C0S1
FP-[U-a]+[CT-BS]+[BS-a(b,ab)] FP-[U-a]+[CT-BS]+[CT-FS] FP-[U-a]+[CT-FS]+[BS-a(b,ab)]	C0S0

TABLE IV: Possible fixed points and phases of the n -component fermion ladder with half-filled subband for $n = 2$.

The phases occurring when the system is half-filled and one or more interband umklapp processes are relevant are listed in Table V for $n > 2$. The umklapp scattering processes—similarly to the charge-transfer processes—open at least one charge and $n - 1$ spin gaps. A soft charge mode may be present in the spectrum only if all charge-transfer processes are irrelevant, moreover, in phase C1S($n - 1$) the umklapp scattering between electrons with parallel spins only may be relevant. As it was

mentioned in the previous section the couplings $g_{3\perp}^{abab}$ and $g_{3\perp}^{abba}$ open $2(n - 1)$ spin gaps, therefore—due to the fully gapped spin sector—the relevance of the processes which open gap in the spin sector only ($g_{1\perp}^a, g_{1\perp}^b, g_{1\perp}^{ab}$) does not modify the spectrum. However, in phase C1S0, besides the coupling $g_{3\parallel}^{ab}$ at least one backward scattering has to be scaled to strong coupling. We note that the charge-transfer umklapp process $g_{3\perp}^{ct}$ alone makes the spectrum fully gapped, but of course in phase C0S0, all couplings may be relevant.

fixed point	phase
FP-TL	C2S2($n - 1$)
FP-U-ab \parallel	C1S($n - 1$)
FP-U-ab \perp FP-[U-ab \parallel]+[BS-a(b,ab)]	C1S0
FP-CT-U FP-[U-ab \perp]+[CT-FS] FP-[U-ab \perp]+[CT-BS] FP-[U-ab \parallel]+[CT-FS] FP-[U-ab \parallel]+[CT-BS]	C0S0

TABLE V: Possible fixed points and phases of the half-filled n -component fermion ladder for $n > 2$.

If $n = 2$ the charge-transfer umklapp processes do not open gap in the spin sector, therefore, new phases—namely C0S2 and C0S1—occur in the phase diagram compared to $n > 2$ (see Table VI). It has to be noted that similarly to $n > 2$ the spin sector can be fully gapped without relevant backward-scattering processes (FP-[U-ab \perp]+[U-ab \parallel]) and the relevance or irrelevance of the non-charge-transfer backward scattering processes does not modify the gap structure. Moreover, in the fixed points, where relevant charge-transfer umklapp processes are present, the relevance of any other coupling leads to phase C0S1 (the last three fixed points for phase C0S1), except for $g_{1\perp}^{ab}$ which opens $2(n - 1)$ spin gaps, so the spectrum becomes fully gapped and the corresponding phase is C0S0.

fixed point	phase
FP-TL	C2S2
FP-U-ab \perp (ab \parallel)	C1S1
FP-[U-ab \perp]+[BS-a(b,ab)] FP-[U-ab \perp]+[U-ab \parallel] FP-[U-ab \parallel]+[BS-a(b,ab)]	C1S0
FP-CT-U	C0S2
FP-[U-ab \perp]+[CT-FS] FP-[U-ab \parallel]+[CT-BS] FP-[CT-U]+[BS-a(b,CT)] FP-[CT-U]+[U-ab \perp (ab \parallel)] FP-[CT-U]+[CT-FS]	C0S1
e.g. FP-[U-ab \perp]+[CT-BS]	C0S0

TABLE VI: Possible fixed points and phases of the half-filled n -component fermion ladder for $n = 2$.

It can be seen that all possible phases have been found if $n = 2$ while for $n > 2$ some theoretically possible phases

do not occur. This is due to the fact mentioned above that in this case there are no couplings which open gap in the charge sector only: a charge gap opens always together with spin gaps. A more complete phase diagram could be obtained if the couplings have a more general spin dependence. Although, even in this case the charge gaps are coupled to spin gaps, it would be possible to open a single spin gap—if the corresponding fixed point exists—contrary to case investigated above where $n - 1$ spin gaps occur always together.

VI. NUMERICAL RESULTS

The behavior close to the weak-coupling fixed point has been analyzed in Sec. IV analytically. A similar calculation close to the strong-coupling fixed points is not possible since—as mentioned earlier—the scaling equations derived in the leading logarithmic approximation are not valid in the strong-coupling regime. The relevance or irrelevance of the couplings could, however, be deduced from the numerical solution of the scaling equations. We have done numerical studies for different band fillings for models in which the bare couplings correspond to a repulsive Hubbard ladder, and also for somewhat more general situations characterized by several bare coupling constants.

A. Hubbard ladder

In a Hubbard ladder the initial couplings of all intraband and interband scattering processes $g_{i\perp}^{\alpha\beta\gamma\delta}$ are related to the same on-site interaction U defined in Eq. (1) while $g_{\parallel}^{\alpha\beta\gamma\delta}$ and $g_{3\parallel}^{ab}$ are equal to zero. The numerical results presented below were obtained for $U/(2\pi\hbar v_a) = 0.1$ and different values for the ratio v_b/v_a . Other choices for $U/(2\pi\hbar v_a)$ gave qualitatively identical results.

1. Generic filling

When the unklapp processes may be neglected 12 scattering processes have to be taken into account. Looking at the lowest-order scaling equations it can be shown that if the initial couplings satisfy the relations

$$g_{1\perp}^{a(b,ab,ct)} = g_{\parallel}^{a(b,ab,ct)} + g_{2\perp}^{a(b,ab,ct)}, \quad (75)$$

what is the case for the Hubbard ladder, the same relations remain valid for the renormalized couplings. Due to these scale-invariant surfaces eight independent couplings describe the system. The second-order scaling curves for these couplings for $v_b/v_a = 1.5$ are shown in Fig. 6.

One can see that all scaling trajectories go to infinity so all couplings are relevant for all value of n . The weak-coupling fixed point, which is stable for the $n = 2$ Hubbard chain, is not reached for the Hubbard ladder.

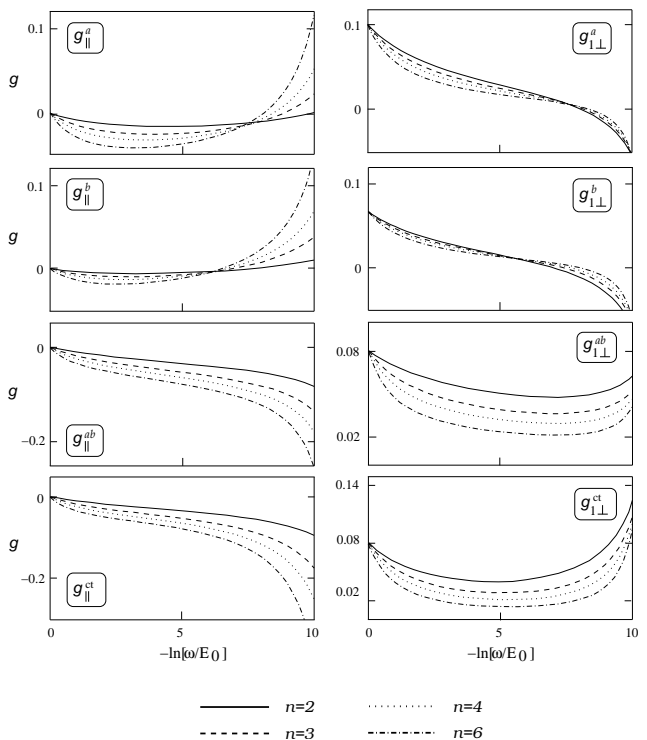


FIG. 6: The second-order scaling curves for a weak-coupling Hubbard ladder ($U/(2\pi\hbar v_a) = 0.1$, $v_b/v_a = 1.5$) for the 8 independent couplings and for different values of n .

Since the backward-scattering and charge-transfer processes are relevant the corresponding phase is C1S0. For generic filling the $SU(n)$ Hubbard ladder is not a Luttinger liquid.

Similar results are obtained for other γ values provided they are of the order of unity. Solving the scaling equations formally for larger values of γ , it was found that successively some of the charge-transfer and backward-scattering processes become irrelevant and new phases occur. Namely, if v_b/v_a or v_a/v_b (since γ takes the same value when v_b/v_a is replaced by v_a/v_b) is approximately 8.3, all charge-transfer processes, the interband backward scattering $g_{1\perp}^{ab}$ and one of the intraband backward-scattering terms $g_{1\perp}^a$ or $g_{1\perp}^b$, belonging to the band with smaller velocity, become irrelevant and FP-BS-b or FP-BS-a is reached. The corresponding phase is C2S($n - 1$). The surviving intraband backscattering $g_{1\perp}^b$ or $g_{1\perp}^a$ becomes irrelevant above an even higher value—approximately 8.7—of the velocity ratio v_b/v_a or v_a/v_b . None of the couplings that could open gap in the spectrum seem to be relevant and the Luttinger liquid phase C2S2($n - 1$) would be obtained. These boundaries vary little with n . These phases appear, however, in such situations where one of the subbands is almost empty or almost full, the curvature of the dispersion relation may be important, and a model with linearized spectrum may not be a good approximation. For this reason these phases are not indicated in the phase diagram.

2. Role of intraband umklapp processes

If $4k_a$ is equal to a reciprocal lattice vector G and the umklapp process $g_{3\perp}^a$ is relevant the surfaces determined by (75) remain invariant. Therefore out of the 13 couplings which give contribution 9 are independent. The scaling curves for these couplings obtained in the leading logarithmic approximation can be seen in Fig. 7.

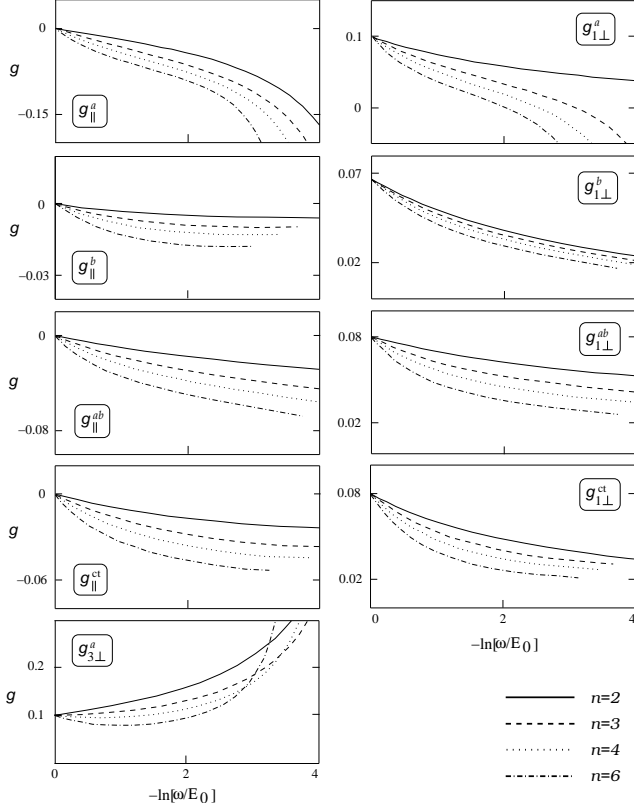


FIG. 7: The second-order scaling curves for the Hubbard ladder ($U/(2\pi\hbar v_a) = 0.1$, $v_b/v_a = 1.5$) with half-filled subband.

It is found that starting from the bare couplings characterizing the Hubbard ladder the weak-coupling fixed point cannot be reached for any value of n and for any value of γ . The strong-coupling fixed point FP-[U-a]+[CT-FS] where the umklapp processes are relevant together with the charge-transfer ones but all backward-scattering processes are irrelevant seems to be accessible for the Hubbard ladder if $n = 2$ (independently of the value of γ). The corresponding phase is C0S1. As has been seen above, this fixed point could not be reached for $n > 2$ and phase C0S0 is realized there. Similar result has been found⁵ for the 1D $SU(n)$ chain where it was shown that the umklapp scattering suppresses the normal backward-scattering processes for $n = 2$ only.

3. Half-filled system: interband umklapp processes

When the whole system is half-filled, the contribution of the interband umklapp processes should be taken into account. The scaling equations are invariant under the interchange of bands a and b

$$g_i^a = g_i^b \quad (76)$$

and therefore out of the 16 coupling which give contribution in a half-filled system, 13 are independent. The scaling curves for these couplings are shown in Fig. 8.

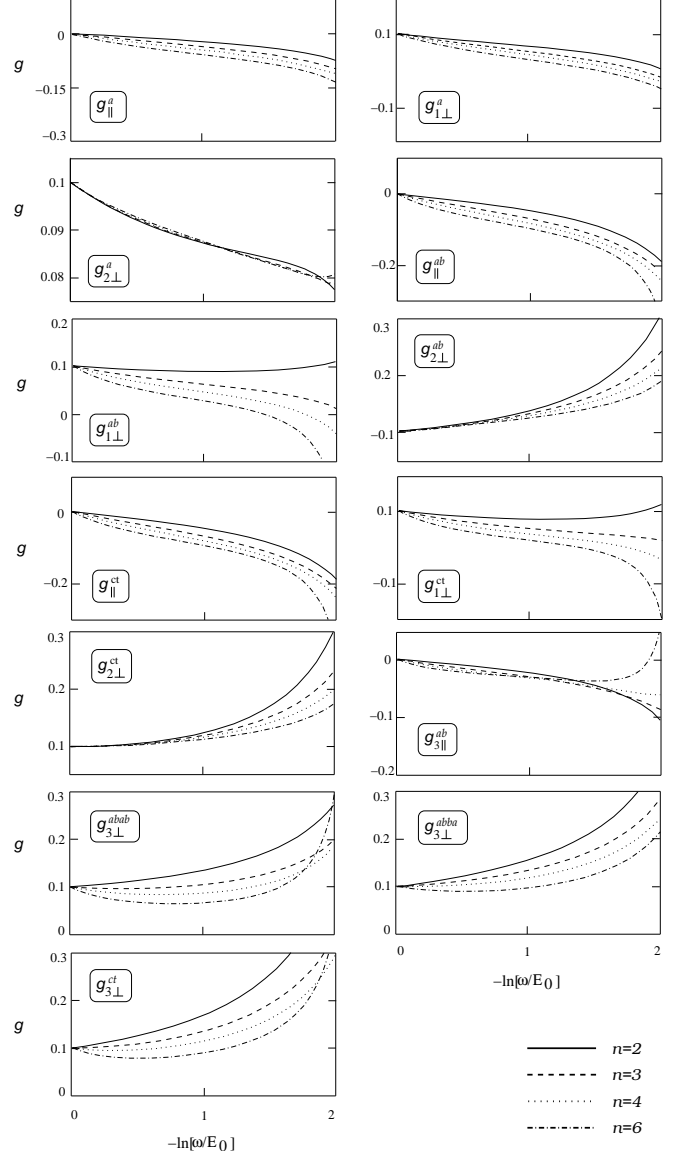


FIG. 8: The second-order scaling curves for the half-filled Hubbard ladder ($U/(2\pi\hbar v_a) = 0.1$).

The weak-coupling fixed point determined by (30), (31) and (38) cannot be reached starting from the Hubbard ladder. Similarly to the case of generic filling, for any n and γ all couplings go to infinity. But since now the

umklapp processes, too, are relevant, the corresponding phase is COS0.

Figure 9 shows the phase diagram of the Hubbard model. The control parameter is the filling n_i/n where n_i is the particle number per site. $n_i/n = 0$ and 1 denote the totally empty and full system, respectively, b_0 denotes the filling when the upper band is almost empty, similarly a_1 denotes the filling when the lower band is almost full. Close to these fillings the linearization of the spectrum is not valid, and the shaded regime around these points indicates that the results presented in this paper using a linearized spectrum may not be reliable at these fillings. For this reason the phases found in these regimes are not indicated in the figure.

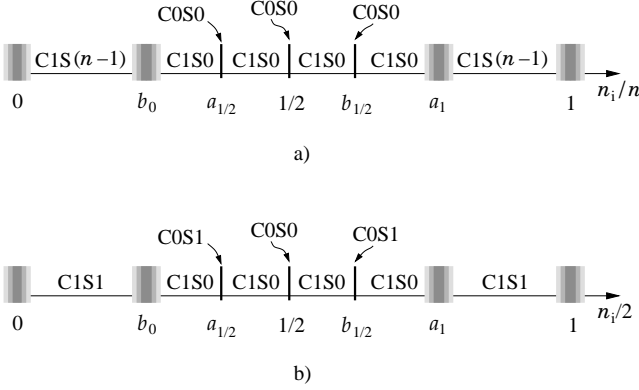


FIG. 9: The phase diagram of the Hubbard ladder: a) for $n > 2$ and b) for $n = 2$.

The upper figure (a) shows the phase diagram of the n -component Hubbard ladder for $n > 2$. Figure (b) is valid for 2-component fermions. As one can see the $n = 2$ and $n > 2$ models behave differently in the presence of intraband umklapp processes.

B. Chains with forward scattering only

As another special case we consider two chains with nonchiral intrachain forward scattering only. Although the interband scattering processes that arise when the one-particle transverse hopping is switched on are all of forward-scattering type, the charge-transfer processes do not conserve the chiral charge and spin. For this reason in general, such a ladder does not behave like a Luttinger liquid.

The couplings which play a role in this coupled system are related to scattering processes between electrons of the same spin: g_{\parallel}^a , g_{\parallel}^b , g_{\parallel}^{ab} and $g_{\parallel}^{\text{ct}}$, and to forward scattering processes between electrons of different spins: $g_{2\perp}^a$, $g_{2\perp}^b$, $g_{2\perp}^{ab}$ and $g_{2\perp}^{\text{ct}}$. The scaling equations for the intraband scatterings are:

$$\frac{dg_{\parallel}^a}{d \ln x} = -\gamma(g_{\parallel}^{\text{ct}})^2, \quad (77a)$$

$$\frac{dg_{2\perp}^a}{d \ln x} = \gamma(g_{2\perp}^{\text{ct}})^2 \quad (77b)$$

Similar equations hold for the couplings in band b . The Lie equations for the interband scatterings without charge transfer are:

$$\frac{dg_{\parallel}^{ab}}{d \ln x} = (g_{\parallel}^{\text{ct}})^2, \quad (78a)$$

$$\frac{dg_{2\perp}^{ab}}{d \ln x} = -(g_{2\perp}^{\text{ct}})^2, \quad (78b)$$

and for the charge-transfer processes

$$\frac{dg_{\parallel}^{\text{ct}}}{d \ln x} = -g_{\parallel}^{\text{ct}} [g_{\parallel}^a + g_{\parallel}^b - 2g_{\parallel}^{ab}], \quad (79a)$$

$$\frac{dg_{2\perp}^{\text{ct}}}{d \ln x} = g_{2\perp}^{\text{ct}} [g_{2\perp}^a + g_{2\perp}^b - 2g_{2\perp}^{ab}]. \quad (79b)$$

As can be seen, the coupling constants of the scattering processes between electrons of the same spin and of different spins are not coupled, the two scattering channels are separated, and analogous equations are obtained.

These equations have one weak-coupling fixed point only, namely when the processes which transfer charge from one band to the other are irrelevant. This fixed “point” is a six-dimensional hypersurface in the parameter space and it can be attractive if

$$2g_{\parallel}^{ab*} \geq g_{\parallel}^{a*} + g_{\parallel}^{b*}, \quad (80a)$$

$$g_{2\perp}^{a*} + g_{2\perp}^{b*} \geq 2g_{2\perp}^{ab*}. \quad (80b)$$

As we have seen in Sec. IV, at this fixed point the system is a Luttinger liquid. One finds, however, different behavior depending on whether the interband scatterings are scaled out of the problem or not. If these processes vanish, the two charge modes become independent, and similarly the spin modes are decoupled, while if the interchain couplings survive, the charge modes become coupled and have identical velocities. Similar situation occurs for the spin modes as well.

The scaling equations have been solved numerically for one-parameter models, i.e., for models characterized by a single bare coupling constant U . According to (23) the dimensionless couplings $g^{\alpha\beta\gamma\delta}$ appearing in the scaling equations are $\tilde{U} = 2U/\pi\hbar(v_{\alpha} + v_{\beta} + v_{\gamma} + v_{\delta})$.

We have found, starting from a one-parameter Hubbard-like model—the Coulomb interaction between electrons of the same spin is zero—that the charge-transfer processes become relevant, the stable fixed point is FP–CT–FS both for fully repulsive and fully attractive models. In fact the sign of the couplings $g_{\parallel}^{\text{ct}}$ and $g_{2\perp}^{\text{ct}}$ is not relevant in this respect, so this strong-coupling fixed point is reached if

$$g_{\parallel}^{a(0)} = g_{\parallel}^{b(0)} = g_{\parallel}^{ab(0)} = g_{\parallel}^{\text{ct}(0)} = 0, \quad (81)$$

and

$$g_{2\perp}^{a(0)} = g_{2\perp}^{b(0)} = g_{2\perp}^{ab(0)} = \pm g_{2\perp}^{\text{ct}(0)} = \pm \tilde{U}. \quad (82)$$

One charge and $n - 1$ spin gaps open in the spectrum, the phase is C1S($n-1$).

Due to the analogous structure of the Lie-equations listed above the same behavior is found if the bare couplings $g_{\parallel}^{(0)}$ are all repulsive or attractive while the bare $g_{2\perp}^{(0)}$ couplings vanish:

$$g_{\parallel}^{a(0)} = g_{\parallel}^{b(0)} = g_{\parallel}^{ab(0)} = \pm g_{\parallel}^{\text{ct}(0)} = \pm \tilde{U} \quad (83)$$

and

$$g_{2\perp}^{a(0)} = g_{2\perp}^{b(0)} = g_{2\perp}^{ab(0)} = \pm g_{2\perp}^{\text{ct}(0)} = 0. \quad (84)$$

Moreover, if the couplings $g_{\parallel}^{(0)}$ or $g_{2\perp}^{(0)}$ are all repulsive or attractive, the gap structure is not modified when some of the other bare couplings appear with opposite sign.

Luttinger liquid behavior could, however, be found when the intraband forward scatterings ($g_{2\perp}^a$ and $g_{2\perp}^b$) are repulsive and the interband forward scattering ($g_{2\perp}^{ab}$) is attractive,

$$g_{\perp}^{(0)} = 0, \quad g_{2\perp}^{a(0)} = g_{2\perp}^{b(0)} = -g_{2\perp}^{ab(0)} = \pm g_{2\perp}^{\text{ct}(0)} = \tilde{U}, \quad (85)$$

since in this case the charge-transfer processes scale to zero. As we have seen in Sec. IV two different velocities appear in the system. Similar situation is encountered if the intraband forward scattering between particles of the same spin is attractive and the intraband forward scattering is repulsive,

$$g_{\perp}^{(0)} = 0, \quad g_{2\parallel}^{a(0)} = g_{2\parallel}^{b(0)} = -g_{2\parallel}^{ab(0)} = \pm g_{2\parallel}^{\text{ct}(0)} = -\tilde{U}. \quad (86)$$

These results are independent of the value of n . Although the Luttinger-liquid behavior with four different velocities is theoretically possible, for the parameter values chosen no such behavior has been found, because even though the charge-transfer processes are scaled out, the interband forward-scattering processes g_{\parallel}^{ab} and $g_{2\perp}^{ab}$ remain finite.

VII. CONCLUSIONS

In the present paper, we have investigated a fermion ladder in which two n -component fermion chains are coupled by interchain hopping. Using the multiplicative renormalization-group procedure we have derived the second order scaling equations, determined the fixed points and analyzed the possible phases.

One weak-coupling fixed point has been found where the system behaves like a Luttinger liquid. In this fixed point, the processes which violate the conservation of the particle number and spin on each branch separately, namely the charge-transfer processes from one band to the other, the backward and the umklapp processes are irrelevant. In the basin of attraction of the Tomonaga-Luttinger fixed point, where all modes, namely the two charge and $2(n - 1)$ spin modes are soft, the Hamiltonian

has been diagonalized for general spin-dependence of the couplings. In this fixed point, different behavior has been found depending on the relevance or irrelevance of the interband forward scatterings. If they are irrelevant the system behaves like two independent Luttinger liquid, $2n$ different velocities characterize the ladder, meaning full mode separation. On the other hand, if the interband scatterings are relevant, this coupling allows for n different velocities only. In the special case when the coupling strength depends on the relative orientation of the spins of the scattered particles, the velocities of all spin modes become equal, and the usual charge-spin separation is recovered.

Besides this weak-coupling fixed point there are several strong-coupling fixed points. The relationship between them and the appropriate phases have been determined by the bosonization treatment. The possible phases for generic filling as well as for half-filled subbands and for a half-filled ladder have been described. Since the exact location of the strong-coupling fixed points cannot be determined in the approximation used, the strong-coupling regime has been investigated numerically. The scaling equations have been solved for some special initial values of the couplings, among others for a Hubbard ladder.

We have found that the generically filled Hubbard ladder has fully gapped spin sector and one gapped charge mode (C1S0), the system does not show Luttinger liquid behavior for any n . The half-filled Hubbard ladder is not Luttinger liquid, either, it has not only fully gapped spin sector but the charge sector, too, is gapped. The phase is C0S0. These results do not depend on the initial value of the Hubbard U , any nonzero value of the Coulomb interaction leads to the same phases.

The $n = 2$ case, the SU(2) Hubbard ladder has been investigated in detailed using similar methods in Refs. 12 and 13. The results agree in that regime where the linearized spectrum is a reasonable approximation. Six of the seven phases predicted in these papers were found by us. The remaining one—as well as two of these six phases—are in that parameter range where our approximation is questionable. Interestingly five of these six phases occur in the phase diagram of the SU(n) Hubbard ladder, too.

The Hubbard ladder with half-filled subband shows special behavior in the case $n = 2$. We have found that in this case the backward scatterings are irrelevant, therefore, there is one soft spin mode in the system (C0S1). On the other hand if $n > 2$ the situation is the same as for a half-filled ladder: all couplings are relevant and the corresponding phase is C0S0, i.e. all modes are gapped. Similar result has been found in our earlier work, for the SU(n) symmetric half-filled Hubbard chain: the half-filled system has gapped charge mode and soft spin mode (phase C0S1) for $n = 2$, while for $n > 2$ the system is fully gapped (phase C0S0). In this sense similar behavior has been found for the weakly coupled Hubbard ladder with half-filled subband and for the half-filled Hubbard chain. This result seems to support the claim⁹ that the intra-

band umklapp processes lead to 'confinement', i.e., to the vanishing of the interchain hopping in a two-component weakly coupled two-leg Hubbard ladder.

Finally we have shown that if two n -component Luttinger chains with repulsive forward scattering are coupled by interchain hopping then—similarly to the case of the coupled generically filled n -component Hubbard chains—the 1D Luttinger liquid state is unstable not only for usual electrons with spin-1/2 but for n -component fermions, too. Luttinger liquid behavior could be obtained if some but not all of the couplings are attractive.

In the present paper, the gapped phases have been characterized by the number of gapped modes only. The study of the correlation functions could reveal further details of the obtained phases.

Acknowledgments

This research was supported in part by the Hungarian Research Fund (OTKA) under Grant No. 43330.

-
- ¹ F. D. M. Haldane, J. Phys. C **14**, 2585 (1981).
² L. H. Lieb and F. Y. Wu, Phys. Rev. Lett. **20**, 1445 (1968).
³ J. B. Marston and I. Affleck, Phys. Rev. B **39**, 11538 (1989).
⁴ R. Assaraf, P. Azaria, M. Caffarel, and P. Lecheminant, Phys. Rev. B **60**, 2299 (1999).
⁵ E. Szirmai and J. Sólyom, Phys. Rev. B **71**, 205108 (2005).
⁶ C. Castellani, C. Di Castro and W. Metzner, Phys. Rev. Lett. **69**, 1703 (1992).
⁷ M. Fabrizio, A. Parola, and E. Tosatti, Phys. Rev. B **46**, 3159 (1992); M. Fabrizio, A. Parola, Phys. Rev. Lett. **70**, 226 (1992); M. Fabrizio, Phys. Rev. B **48**, 15838 (1993).
⁸ D. Boies, C. Bourbonnais, and A.-M. S. Tremblay, Phys. Rev. Lett. **74**, 968 (1995); Proc. XXXI Rencontres de Moriond, Eds.: T. Martin, G. Montambaux, J. Tran Thanh (1996).
⁹ K. Le Hur, Phys. Rev. B **63**, 165110 (2001).
¹⁰ D. V. Khveshchenko and T. M. Rice, Phys. Rev. B **50**, 252 (1993).
¹¹ H. J. Schulz, Phys. Rev. B **53**, R2959 (1996).
¹² L. Balents and M. P. A. Fisher, Phys. Rev. B **53**, 12133 (1996).
¹³ H.-H. Lin, L. Balents, and M. P. A. Fisher, Phys. Rev. B **58**, 1794 (1998).
¹⁴ C. Wu, W. V. Liu, and E. Fradkin, Phys. Rev. B **68**, 115104 (2003).
¹⁵ G. Abramovici, J. C. Nickel, and M. Héritier, Phys. Rev. B **72**, 045120 (2005).
¹⁶ K. Penc and J. Sólyom, Phys. Rev. B **41**, 704 (1990).
¹⁷ E. Dagotto, J. Riera, and D. J. Scalapino, Phys. Rev. B **45**, 5744 (1992).
¹⁸ D. Poilblanc, H. Endres, F. Mila, M. G. Zacher, S. Capponi, and W. Hanke, cond-mat/9605106.
¹⁹ D. J. Scalapino, J. Low Temp. Phys. **117**, 179 (1999).
²⁰ R. M. Noack, S. R. White and D. J. Scalapino, Phys. Rev. Lett. **73**, 882 (1994).
²¹ Y. Park, S. Liang and T. K. Lee, Phys. Rev. B **59**, 2587 (1999).
²² U. Schollwöck, S. Chakravarty, J. O. Fjærestad, J. B. Marston and M. Troyer, Phys. Rev. Lett. **90**, 186401 (2003).
²³ A. V. Rozhkov, Phys. Rev. B **68**, 115108 (2003).
²⁴ S. C. Zhang, Science **275**, 1089 (1997).
²⁵ D. G. Shelton and D. Sunchal, cond-mat/9710251.
²⁶ M. Tsuchiizu and A. Furusaki, Phys. Rev. B **66**, 245106 (2002).
²⁷ C. Honerkamp and W. Hofstetter, Phys. Rev. Lett. **92**, 170403 (2004).
²⁸ J. Sólyom, Adv. Phys. **28**, 201 (1979).
²⁹ S. Ledowski, P. Kopietz and A. Ferraz, cond-mat/0412620.